DIRECTIONAL RECRYSTALLISATION IN DISPERSION STRENGTHENED ALLOYS

by

Muhammad Moazam Baloch

Clare College

Cambridge

A dissertation submitted for the fulfilment

of the Degree of Doctor of Philosophy

at the University of Cambridge

October 1989

PREFACE

The work described in this dissertation was carried out in the Phase Transformations Group at the Department of Materials Science and Metallurgy, University of Cambridge, between October 1986 and October 1989 under the supervision of Dr. H. K. D. H. Bhadeshia. The work presented in this dissertation is original and includes nothing which is the outcome of work done in collaboration, except where acknowledgement and reference to previous work has been made. This dissertation is less than 60,000 words long and has not been submitted for any degree, diploma or other academic qualification at any other university.

M. M. BALOCH
October 1989.

ACKNOWLEDGEMENTS

To
Erum and Asad

ABSTRACT

Conventional recrystallisation heat treatments lead ultimately to a microstructure consisting of equiaxed grains. There is now an industrial demand for the production of highly anisotropic grain microstructures by solid-state processing, rather than by the more usual directional solidification routes. The latter do not seem to be suitable for certain applications, including the fabrication of wafers with elongated grains.

This thesis deals with an investigation of directional recrystallisation, a solid-state process in which heavily deformed metallic samples are recrystallised to yield highly anisotropic, directional grain microstructures. The aim of the project was to investigate the the fundamental metallurgy of this particular process, and to model the process itself.

The study includes mechanically alloyed superalloy of the kind used in the aircraft industry, mechanically alloyed ferritic stainless steels, rapidly solidified and compacted aluminium alloys and aluminium alloys produced by other routes. With one exception all the alloys used are in some way dispersion strengthened, so that the energy stored due to deformation can be very high. All the alloys were obtained from external suppliers, either as standard commercial alloys, or as experimental alloys. Since some of the alloys have a high intrinsic strength, they were deformed at temperatures as high as 1000°C.

Directional recrystallisation was induced by using an experimental technique, in which, deformed samples are in effect subjected to a moving heat source which leads to a recrystallisation in a temperature gradient.

The microstructure of the as-extruded samples was found to reflect a typical deformation structure, with flattened grains containing a high density of dislocations. The alloys readily directionally recrystallised, but the direction of the major axes of the grains was always found to be roughly parallel to the extrusion direction, irrespective of the sense of the imposed temperature gradient. Indeed, even isothermal annealing led to a directionally recrystallised microstructure. Detailed investigations revealed two main causes for this behaviour: The oxide particles in the alloy were found to be strongly aligned along the extrusion direction, and a measurement of stored energy revealed that the driving force for recrystallisation was very large, making it difficult to controll the process. This latter difficulty could be overcome by pre-annealing at relatively low temperatures to reduce the stored energy.

By contrast, the superalloy which has a rather low level of stored energy, did not undergo directional recrystallisation during isothermal heat treatment, and the recrystallisation behaviour changed with the relative direction of the imposed temperature gradient with respect to the extrusion direction. Detailed metallography and crystallography revealed that the alloys had, during deformation, undergone primary recrystallisation to an ultra fine grained microstructure, which accounted for most of the stored energy. The directional recrystallisation observed was therefore, a secondary recrystallisation process.

The results of the experiments of the steels are rationalised using the concept of kinetic strength of a heat treatment, and a model is developed and used to measure the mobility of interfaces.

The experiments on the aluminium alloys were not successful in producing directional structures and the reasons for this behaviour are discussed.

CONTENTS

Chapter Four:

Characterisation of As-Deformed Microstructure of ODS Nickel Base Superalloy (MA6000) and ODS Ferritic Steel (MA956)

Chapter Five:

Zone Annealing and Isothermal Annealing Experiments Performed on Oxide Dispersion Strengthened Nickel Base Superalloy Inconel MA6000

Chapter Six:

Zone Annealing and Isothermal Annealing Experiments Performed on Oxide Dispersion Strengthened Ferritic Steel Incoloy MA956

Chapter Seven:

Zone Annealing and Isothermal Annealing Experiments on Oxide Dispersion Strengthened Ferritic Steel Incoloy MA956

CHAPTER ONE

Introduction

1.1 Background to project

The need to improve the performance and efficiency of gas turbine engines, in particular their high-temperature capabilities, has led to the continuing development of materials with higher strength, better corrosion resistance and greater ease of fabrication. Oxide dispersion strengthened (ODS) alloys are promising candidates for use in components in some of hotter parts of the gas turbines.

There are, essentially, two major classes of gas turbines: aircraft engines and industrial ground based gas turbines. Industrial gas turbines are much larger than aircraft engines and are expected to have a life time about ten times that of aircraft engines (Singer, 1986). Industrial gas turbines are also expected to run in much more corrosive conditions and using lower grades of fuel. While alloy development for both types of turbines follows similar lines, there are some important differences. For instance, the increased size of the blades and vanes in industrial gas turbines means that it is not possible to easily apply the single crystal technology of the smaller aircraft engine components. Therefore, in order to achieve improvements in high-temperature performance over that provided by conventionally cast blades, ODS alloys must be considered as promising alternatives.

The utilisation of ODS alloys in aircraft gas turbines in large quantities will require an enormous amount of research before the alloys are taken seriously. However, they are already used commercially for combustion chamber components and as guide-vane materials (Crowford, 1983).

1.2 Scope and Aim of project

The thermodynamic efficiency of a jet engine depends on the difference between the maximum and minimum temperature involved in its thermal cycle. It is in fact given by $(T_{max} - T_{min}) / T_{min}$, where the temperatures are absolute temperatures. Raising the operating temperature can therefore lead to an increase in efficiency. Current maximum operating temperatures are around 1000°C.

This project deals with an aspect of a novel and speculative method for designing metallic turbine blade materials for operation at temperatures as high as 1400°C. It is envisaged that a blade would be constructed of a series of thin wafers, with very efficient cooling channels to ensure that the blade material will be maintained at 1000°C, while the environment is at 1400°C. Many turbine blades in current use already have cooling channels machined or cast into position, but these are usually narrow and not sufficiently efficient in the present context.

For reasons of creep resistance the wafers discussed above need to have a directional grain microstructure, which cannot be produced by directional solidification, as is usual for bulk alloys.

This project deals with the modelling of a solid-state process of directional recrystallisation which should lead to the required creep resistance microstructure in thin wafers. The chemical compositions of the model materials investigated are given in Table 3.1. In this thesis fundamental phenomenon like recovery, recrystallisation and grain growth are briefly reviewed in chapter two and chapter three discusses the details of experimental techniques, fabrication of the alloys used to study directional recrystallisation.

Although the mechanism of directional recrystallisation is not fully understood, it intuitively seems essential that the starting deformed material has a large quantity of stored free energy. Furthermore, it seems that directional recrystallisation occurs only if the rate of release of stored free energy is high during annealing. In order to achieve a high level of stored free energy due to deformation, and to reduce dynamic recovery, oxide dispersion strengthened materials are used for directional recrystallisation. The oxide particles also help to induce the rapid multiplication and accumulation of defects during deformation. Therefore, initial microstructures of oxide dispersion strengthened alloys MA6000 and MA956 has been characterised by transmission electron microscopy, in terms of grain size measurements and the orientation relationship between two adjacent grains in the deformed condition and are discussed in chapter four.

There are two general techniques for producing elongated grain microstructures, One method, known as directional solidification (D.S) involves controlling the heat flow and other conditions during the solidification process to produce an elongated solidification microstructure. The disadvantage of directionally solidified material is that, it cannot easily be used for very thin sections.

The second method, involves controlled recrystallisation after deformation. In its best known form, this type of process involves straining the material to a critical level which leads to a

presumably critical level of stored energy, and then heating to above the "recrystallisation temperature" under conditions which encourage directional grain growth rather than profuse grain nucleation. This process produces elongated grains in an initially deformed microstructure. The heating is usually performed in a moving thermal gradient and the recrystallised grains tend to grow along the direction of the gradient (Allen et al., 1976). Chapter five deals with the directional recrystallisation behaviour observed after zone annealing oxide dispersion strengthened nickel base superalloy MA6000. The final chapters deal with the results of experimental work: chapter six and seven report a series of exploratory investigations on the directional recrystallisation behaviour of oxide dispersion strengthened ferritic stainless steels MA956 and MA957 respectively, the part played by the oxide particles during recrystallisation of these alloys, and include a model developed for solid-state process of directional recrystallisation has also been discussed.

Discussion specific to each set of results is included in the relevant chapters. Then in chapter eight, all experimental findings are collected and summarised. In the present research an attempt has also been made to directionally recrystallise the aluminium alloys produced by different processes, but none of those aluminium alloys behaved positively towards directional recrystallisation. Therefore, the results obtained after the performance of zone annealing experiments on aluminium alloys are reported in appendix one and two.

CHAPTER TWO

Literature Review

2.1 Introduction

In the first part of this chapter the basic phenomena of recovery, recrystallisation and grain growth are reviewed briefly. Attention is then focused on the development of strong alloys by mechanical alloying. Finally the production, properties and applications of nickel base superalloy (MA6000) and ferritic stainless steel (MA956) used for present work is reviewed.

2.2 Recovery

When a metal is plastically deformed by cold-working, a certain fraction of the mechanical energy which is expended during the deformation process is retained or stored in the metal in the form of various types of imperfections (i.e., vacancies, interstitials, dislocations etc), while the remainder is converted into heat (Titchener & Bever, 1958). The energy thus stored in the metal, renders it thermodynamically unstable with respect to the unstrained, well-annealed condition. If the temperature is high enough to permit reasonable atomic mobility, there will be a tendency for the deformed metal to return again to a lower free energy or the annealed state. Accompanying such an approach towards an equilibrium state will be a release of the stored deformation free energy from the metal. The variety of processes by which the annealed state is reached are classified into two categories, recovery and recrystallisation (Vandermeer & Gordon, 1963).

2.2.1 Kinetics of Recovery

Byrne (1965) has explained the kinetics of recovery as the rate of recovery of a property from its cold-worked value depending on the instantaneous value of that property; it is known that the rate of recovery is a decreasing function of time. Another way of saying this is that, there is no incubation time involved such as that exhibited by the horizontal portion of curve A of figure 2.1.

A finite rate of recovery exists immediately on the start of an isothermal annealing as exhibited by curve B. This proves to be an important difference from the process of recrystallisation which does exhibit an apparent incubation period. Curve B is called an exponential decay curve, since if we call x the instantaneous value of some property in cold-worked condition, and if the rate of

decay of x depends on x we have,

$$dx/dt = -kx \qquad .....(2.1)$$

$$dx/x = -kdt \qquad .....(2.2)$$

$$\ln x = -kt + \text{constant} \qquad .....(2.3)$$

$$x = e^{-kt}e^{\text{constant}} = k_1 e^{-kt} \qquad .....(2.4)$$

Equation 2.4 is an exponential decay curve and this is not the only type of decay observed during recovery. If equation 2.1 were strictly obeyed, then two specimens of very different cold-work histories should, at a given value of x during annealing at the same temperature, have the same decay rate dx/dt. Actually it is usually found that at a given value of x, dx/dt is less for a sample which had the greater amount of cold-work at the start of recovery. If, in equation 2.1, we regard x as the intensity of lattice imperfections responsible for the property changes, then k can represent the probability that one imperfection disappears in a unit time.

i.e.,
$$k = Ke^{-(Q/RT)} \qquad .....(2.5)$$

Where Q is an activation free energy and K is a constant, R is the Universal gas constant and T is the absolute temperature. Putting equation 2.5 into 2.1 and integrating between the limits of x_o to x, we obtain the following results,

$$dx/x = -Ke^{-(Q/RT)}dt \qquad .....(2.6)$$

$$(\ln x)^{x}_{x_o} = -Ke^{-(Q/RT)} \qquad .....(2.7)$$

$$\ln \{x_o/x\} = -Ke^{-(Q/RT)}t \qquad .....(2.8)$$

which reduces to a first order equation (2.9) when T is constant and if Q is not a function of x

$$\ln x_o/x = Ct \qquad \qquad .....(2.9)$$

Several investigations on single crystals of zinc (Cottrell & Aytekin, 1950) and aluminium (Kuhlman et al., 1949) have shown that the increment of x of a physical or mechanical property above that of the deformed metal is related logarithmically to "t" the time of recovery, so that

i.e., $$x = b - a \ln t \qquad \qquad .....(2.10)$$

where "a" and "b" are constants

and $$dx / dt = - a / t \qquad \qquad .....(2.11)$$

Equation (2.11) shows that the rate of change of the property is inversely proportional to the time, and is most rapid at the beginning of the recovery process. This behaviour has been confirmed experimentally for several different physical and mechanical properties, but particularly for the yield stress and electrical resistivity (Honeycombe, 1984).

The rate of recovery increases with increasing temperature, since recovery is a thermally activated process. If an activation energy can be found for a given process, it may be possible to deduce the mechanism by which the process occurs. However, an interesting question is whether or not the activation energy for recovery is a function of time during isothermal annealing (Byrne, 1965).

It has also been suggested by Byrne (1965), that the activation free energy for recovery is the activation free energy for self-diffusion less the stored energy of cold-work. An apparent difficulty with this idea at first glance is that typical reported values of stored energy on a molar basis are about 1/100 of typical self-diffusion activation energies, so the question arises as to how the stored free energy can have any significant influence. One answer to this is that the stored free energy of cold-work is not distributed homogeneously in a material, so that it is quite possible that in some local regions recovery takes place with an activation energy $(Q_{self-diffusion} - Q_{stored})$. In the specimen as a whole, some amount of Q_{stored} must be retained after recovery if the specimen is to recrystallise.
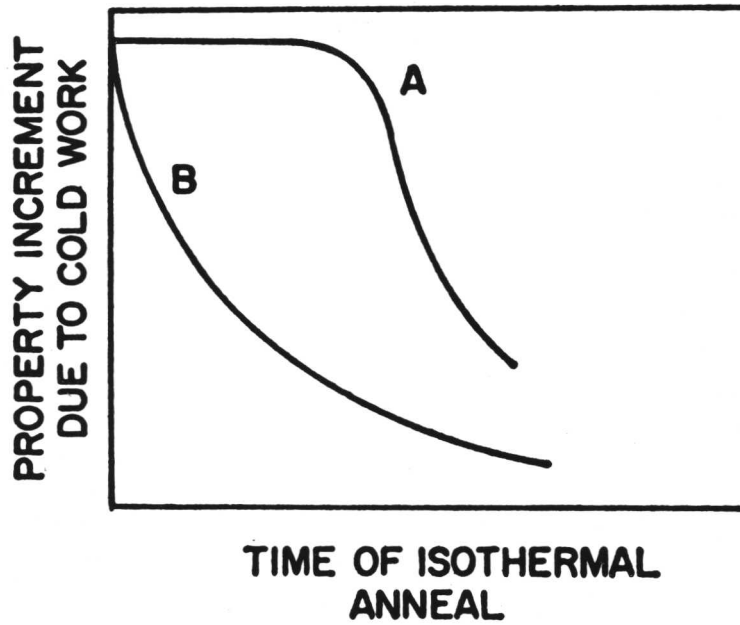
Figure 2.1. Property increment due to cold-work versus time of isothermal anneal. (A) incubation period typical of recrystallisation. (B) Typical decay during recovery (after Byrne, 1965).
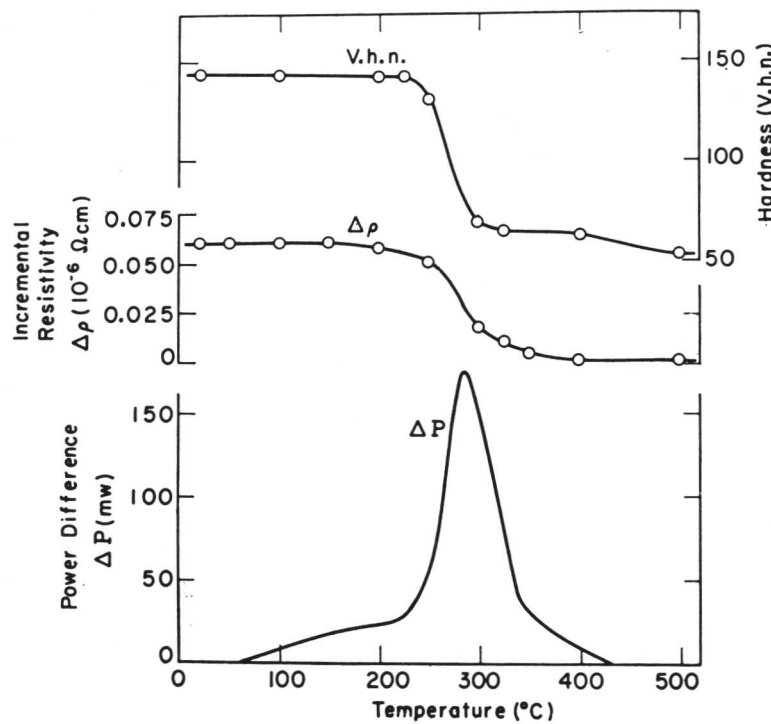
Figure 2.2. Power differential, representing released energy during the uniform heating of plastically twisted copper rod. Recovery of resistivity and hardness are also shown (after Clarebrough et al., 1955).

7

2.3 Release of Stored Internal Energy

When a piece of metal is plastically deformed, a certain amount of external work has to be expended in the process. A small fraction of this work is retained as stored energy, and on annealing the metal, much or all of this is progressively released in the form of heat. The measurements of released heat require highly sensitive differential calorimeters. These calorimeters usually operate at steadily rising temperatures (Clarebrough et al., 1955) or isothermally (Gordon, 1955). In a series of experiments Clarebrough et al. (1955), have determined the stages of the release of stored energy for copper and nickel. As shown in figure 2.2 some of their results correlate the energy release with the change of other physical properties. Pure copper gives off little energy during its recovery stage; only 3-10% of the total stored energy is released, depending on the amount of pre-strain. In nickel, vacancies do not diffuse as readily as in copper, and here the disappearance of vacancies is represented by the region below about 200°C. In figure 2.3 the second small peak represents a form of recovery of uncertain origin. Bell and Krisement (1962), regard the small peak as a beginning of the recrystallisation process. Further evidence, (summarised by Clarebrough et al., 1963) suggests that this stage is connected in some way with the presence of impurities, which slow down the motion of vacancies.

The energy released during the recovery of aluminium must be due entirely to dislocation rearrangements and the formation of cell structures, since vacancies should all have migrated out of the lattice at room temperature. Experimental results such as those in figure 2.3 can be combined with theoretical values for the density, resistivity and stored energy associated with individual vacancies and dislocations, and estimates made of the concentration of these defects in the original deformed material; the overlapping data permit useful cross-checks (Cahn, 1965).

According to Clarebrough et al. (1963), it is now thought probable that the least part of energy release during the recovery stage is due to changes in the arrangement of dislocations, with or without the formation of cell structure. This consideration complicates the calculation of vacancy and dislocation concentrations from the calorimetric measurements. In nickel the energy E_{ry} released in recovery is about the same or 3 times greater than the energy E_{rn} released during recrystallisation (Bell & Krisement, 1962 and Bell, 1965).

In aluminium, the proportion of energy released during recovery is again about equal to that released in recrystallisation. In fact the fraction E_{ry}/E_{rn} is an inverse function of the specific energy of stacking faults on the {111} planes of f.c.c metals. The lower the stacking fault energy, the more

8

difficulty dislocations have in climbing out of their glide planes, an important process in recovery, and the more recovery process is inhibited. In metals with a low stacking fault energy, recovery is limited to the diffusion of vacancies out of the deformed metal; dislocations are not substantially rearranged or eliminated until the beginning of the recrystallisation (Cahn, 1965).

2.3.1 Recovery of Microstructure

Polygonisation

A specially simple form of structural recovery is observed when a crystal is bent in such a way that only a single glide system operates, and is subsequently annealed. The crystal "breaks up" into a number of strain-free subgrains, each preserving the local orientation of the original bent crystal and separated by the plane sub-boundaries which are normal to the glide vector of the active glide plane. This process is termed as polygonisation, because a smoothly curved line in the crystal turns into part of a polygon. This process has been reviewed by Hibbard & Dunn (1957) and Li, (1961). Cahn (1949-50), used this term to describe the edge dislocation walls during the annealing of bent single crystals. Crystals of zinc, aluminium, magnesium and sodium chloride were bent about an axis parallel to their active slip planes. Transmission Laue patterns from these crystals taken with the X-ray beam normal to the bent planes showed the expected continuous asterisms, but when a bent crystal was then annealed close to its melting point and a second Laue pattern taken, the asterism became discontinuous. Cahn (1950), explained the breakup of asterism as due to the formation of walls of dislocations perpendicular to the glide planes as shown schematically in figure 2.4.

To understand the process, it must be recognised that the effect of bending the crystal is to introduce a number of excess dislocations of one sign into the crystal to accommodate the curvature. Thus the large difference in dimension between the outer and inner surfaces of a bent crystal implies the presence of many extra lattice planes near the outer surface which terminate at edge dislocations within the crystal. Upon annealing, these dislocations rearrange themselves into walls of the boundaries which have a lower total elastic strain energy than the more random dislocation arrangement, and this lowering of strain energy provides the driving force for the process. Both climb and glide of edge dislocations is required to form the walls, and these processes require thermal activation, which determines the rate of polygonisation. Gilman (1955) made the first quantitative study of polygonisation and found the average angle of the polygon walls to vary

9

linearly with the logarithm of time at each temperature. Owing to the application of electron microscopy to the study of dislocation distributions in metals, it is now recognised that polygonisation is a special form of sub-boundary formation. Most sub-boundaries are formed during deformation, and are called "cell walls". During annealing the dislocation distribution within the walls becomes more regular. A detailed analysis of the distribution of dislocations in the recovered structure of a two-phase copper crystals has been made by Humphreys and Martin (1967), who studied deformed and annealed specimens in the electron microscope from crystals sectioned in a known relation to the active slip systems. Two copper based systems have been studied in this context: copper-cobalt and copper-silica (where the dispersion of silica is produced by the internal oxidation of a dilute copper-silicon alloy). In both systems, a dispersed phase was produced which was of equiaxed form and of high dimensional stability over extended annealing periods, and the results of annealing at 700°C were dependent upon the stage of deformation of the crystal. According to Humphreys and Martin (1967) none of the two phase crystals recrystallised, but they all recovered, within a few minutes, to structures consisting of networks.

2.4 Recrystallisation

Optimisation of grain structure is important in many cases to achieve desired properties e.g., superplasticity requires fine-grained material, whereas large grains or single crystals may be desired for creep-resistance.

If a cold-worked material is annealed, new strain-free grains may form and replace the original grain structure. This process is known as primary recrystallisation and proceeds by migration of high angle grain boundaries. Further annealing leads to coarsening of the recrystallised grains i.e., grain growth (Rollason, 1961).

2.4.1 Mechanism of Recrystallisation

The plastic deformation of many metals produces internal stresses and alters the electrical conductivity as well as the magnetic permeability of the material, and various other properties.

The effect of heating to different temperatures on the room temperature properties and the change that occurs in grain structure is shown in figure 2.5 for a pure metal. As the temperature is first increased, no change in microstructure can be detected and the strength properties are not significantly affected. However, the electrical conductivity and magnetic permeability increase during the early stages of heating.

10
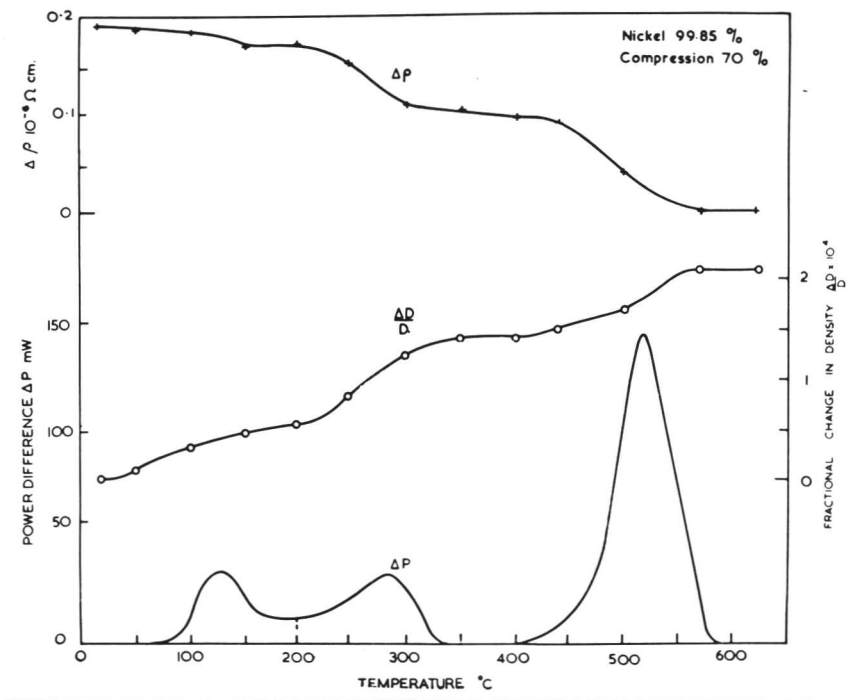
Figure 2.3. Release of stored energy (ΔP), change in extra resistivity (Δe) and the fractional change in density (ΔD/D), for 99.85wt% Ni, deformed 70% in compression and annealed to various temperatures (after Clarebrough et al., 1963).
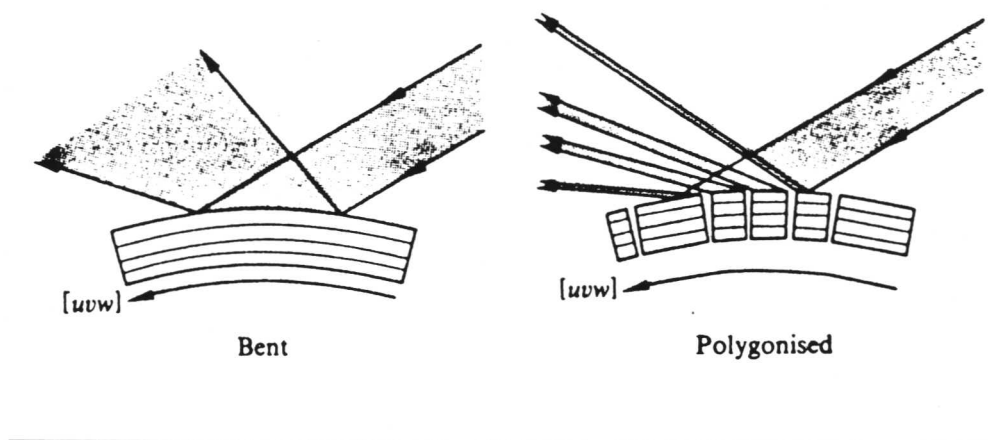
Figure 2.4. Reflection of white radiation by bent and polygonised lattices (after Cahn, 1950).

Furthermore, internal stresses are markedly decreased during this period. As shown in figure 2.5, at the temperature corresponding to point (a), the severely deformed grains are replaced gradually by stress free grains. At the temperature corresponding to point (b) in figure 2.5, the metal is essentially free of internal stresses, and the structure consists of entirely of a very small equiaxed, stress free grains. The temperature interval between points (a) and (b) is a zone of recrystallisation.

The recrystallisation temperature is conventionally defined as the lowest temperature at which equiaxed, stress free grains appear in the microstructure of a previously plastically deformed metal after annealing for a specified time period. The recrystallisation temperature depends upon several factors, the principal ones of which are as follows:

1. The severity of plastic deformation.

2. The grain size prior to plastic deformation.

3. The temperature at which plastic deformation occurs.

4. The time for which the plastically deformed metal is heated to attain recrystallisation.

5. The presence of dissolved or undissolved elements.

The extent to which the degree of plastic deformation influences the recrystallisation temperature of electrolytic iron, low-carbon steel and cartridge brass is shown in figure 2.6.

This figure 2.6, shows that the greater the amount of plastic deformation, the lower the recrystallisation temperature. The finer the grain size, prior to plastic deformation, the lower will be the temperature of recrystallisation. The lower the temperature at which plastic deformation occurs, the lower the temperature of recrystallisation. Longer times at the temperature to which a plastically deformed material is heated lead to a lower recrystallisation temperature. If, for example, a metal is deformed to a certain degree and heated to a particular temperature for 15 minutes, no evidence of recrystallisation may be observed. If it is held for 2 or 3 hours at the same temperature, recrystallisation may be noted. On the other hand, if the same metal, plastically deformed to the same degree and heated to a somewhat higher temperature, complete recrystallisation may be observed in a shorter time. This illustrates the effect of temperature and time upon the recrystallisation process. Soluble impurities and alloying elements generally increase the temperature of recrystallisation. Insoluble impurities are expected to inhibit grain boundary motion and hence may retard recrystallisation and grain growth (Clark and Varney, 1962).

The most highly developed and valid theory for recrystallisation is Cahn's (1950). In Cahn's theory, strain-free regions of small size form by polygonisation in the early stages of annealing. This

12

is not a nucleation process in the true sense, but occurs by thermally activated dislocation rearrangement. The apparent incubation period obtained by extrapolation of experimental curves like that shown in figure 2.7 is not the time to form a nucleus but it is an indication of an initial period of slow growth. In a sense, recrystallisation is now only a growth process, although the operational definition of the nucleation rate remains valid (Christian, 1965). The reasons for the increase of growth velocity with size have been elaborated by Cottrell (1953). According to Cottrell, the initial boundary between a growing region and its surroundings will be of a low energy type interface and hence may be immobile, except in the special circumstances where a glissile boundary is possible. As the boundary moves outwards it collects up individual dislocations and the orientation of the surrounding matrix deviates (tangles cell walls), increasingly from that of recrystallised region. When this misorientation becomes sufficiently large a high angle boundary of relatively great mobility has been formed. This theory emphasises the importance of the variables giving boundary migration rates, not only for grain growth at the later stages of recrystallisation but also throughout the recrystallisation process.

2.4.2 Kinetics of Recrystallisation

The kinetics of recrystallisation are very dependent on a large number of external variables, the most important of which are probably the amount of pre-strain, the purity of material and the orientation difference between a recrystallising grain and the matrix into which it is growing. A minimum amount of deformation is necessary before recrystallisation can be produced, implying driving force and also that recrystallisation may not happen if recovery processes reduce the stored energy below a critical level. The recrystallisation rate is, of course, temperature and time dependent, but the temperature at which this becomes appreciable and the time required to complete the recrystallisation both decrease with increasing amounts of deformation. The structure of a metal prior to deformation is also important: a deformed fine-grained metal recrystallises more readily than a coarse-grained material (Christian, 1965).

2.4.3 Secondary Recrystallisation

The process of secondary recrystallisation has been described by a number of authors such as, Cahn (1950), Clark & Verney (1962), and Cahn (1965). But the secondary recrystallisation process can always be described as when the annealing of an initially deformed sample is continued long beyond the stage when primary recrystallisation is complete. The even tenor of grain growth may be

13
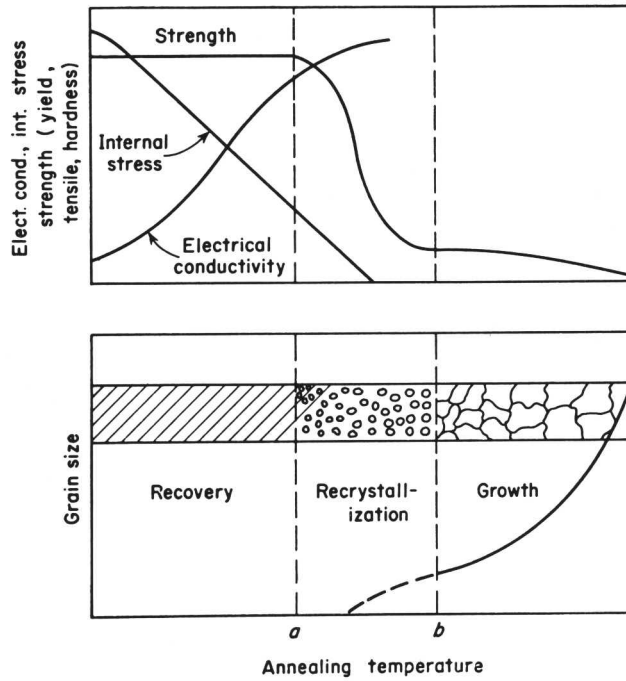
Figure 2.5. The effect of heating a plastically deformed metal on grain size and hardness (after Clark and Varney, 1962).
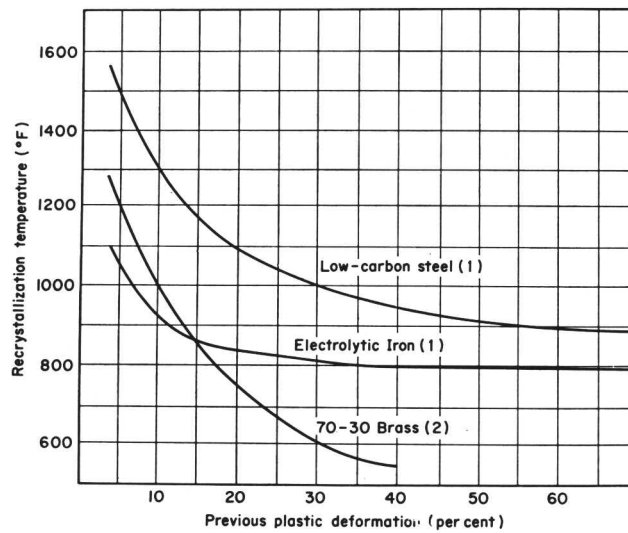
Figure 2.6. The effect of amount of plastic deformation on recrystallisation of iron-steel and brass (after Clark and Varney, 1962).

interrupted by the sudden very rapid growth of a few grains only, to dimensions which may be of the order of centimetres, while the rest of the grains remain small and are eventually all swallowed by the larger grains. This process is known as secondary recrystallisation. The process has the following general characteristics;

(a) The large grains are not freshly formed; they are merely particular grains of the primary structure that have grown large.

(b) The first stage of the growth of the large grains is sluggish; there is an induction period before secondary recrystallisation gets under way.

(c) The factors governing the choice of victorious primary grains which are to grow large, and the mechanism of the early stages are the least understood parts of the process. It is generally agreed that the secondary grains must be appreciably larger than the primary grain size, and must have orientations which diverge from the main primary texture.

(d) Something must inhibit normal uniform grain growth; it is only when the grain growth is very slow that large secondary grains can effectively grow. Inhibition by a dispersed phase, by primary texture or by sheet thickness may all play a part.

(e) The secondary texture, when complete, sometimes has a pronounced texture. Such a texture always differs from the previous primary texture.

(f) A well-defined minimum temperature must be exceeded for secondary recrystallisation. The largest grains are normally produced just above this temperature; at higher annealing temperatures smaller secondary grains are formed.

(g) Once the large grains are well launched the driving force for recrystallisation normally arises from grain boundary energy, (just as in normal grain growth); under special circumstances, the surface energy of the grains can contribute. Figure 2.8 shows several of these regularities (Cahn, 1983).

2.4.4 Factors Effecting Recrystallisation

Contrary to common belief, increasing the number of inclusions present in metallic materials can sometimes increase the rate of isothermal recrystallisation (Leslie et al., 1963). According to Leslie et al., the condition for this to be true is that the growth begins at each inclusion. The function of inclusions, or second-phase particles was assumed to provide regions in which the lattice is relatively undeformed and surrounding by highly deformed material. In addition, the inclusions

provide interfaces which can serve as sinks for the line and point defects during annealing. An example of second-phase particles which contribute to rapid recrystallisation are the cementite particles in low-carbon steels.

If precipitates are made to form after cold-work but prior to recrystallisation, they usually form heterogeneously at prior grain boundaries and dislocation cell walls. During annealing, the precipitates act as barriers, preventing many of the cells from growing and obstructing the movement of prior grain boundaries. This, of course, in general leads to the formation of elongated recrystallised grains, a reduction in the rate of recrystallisation, and a tendency for the cold-worked texture to remain unchanged. If the effects of precipitation prior to cold-work are now considered, a distinction must be made between finely dispersed precipitates and coarse, widely dispersed precipitates (Byrne, 1965).

Leslie et al. (1963), reported that in an iron 0.8 vol% copper alloy given a precipitation treatment prior to cold-work, rod-shaped copper particles formed preferentially at grain boundaries, while other particles were associated with dislocations. When this material was cold-rolled to 60% reduction, a much less clearly defined cell structure resulted. Upon annealing this material, cell formation was inhibited and a very uniform dislocation distribution was produced due to the fact that copper particles, which had deformed, reconstituted themselves into chains of nearly spherical particles along the traces of the initially elongated particles.

2.4.5 Behaviour of Dispersed Particles during Recrystallisation

If an alloy containing particles of a second-phase, is plastically deformed there are two basic ways in which the particles can behave:

(a) The dislocations in the matrix can run through the particles, splitting them by the operation of slip systems and after a high degree of deformation lead virtually to the solution of particles.

(b) The particles possess mechanical properties such that they cannot be deformed (Koster, 1971).

Many high-temperature high-strength alloys such as SAP (sintered aluminium powder) or TD nickel (thoria dispersed nickel) have a microstructure consisting of a matrix containing a high degree of dislocations and a finely divided dispersed second-phase. As a rule, a hardened material of this type recrystallises at a higher temperature and thus rapidly lo ses its hardness. To maintain strength at high temperature, the dispersed phase must retard recrystallisation of the matrix. The

16

recrystallisation behaviour of such materials is thus of great technical interest.

Compared with the behaviour of the matrix without particles, the dispersed particles can cause either an acceleration or a retardation of recrystallisation.

The phenomenon can be explained in general terms by considering that the particles will have the effect of increasing the dislocation density when the specimen is plastically deformed thus increasing the driving force for recrystallisation. On the other hand the particles hinder both the rearrangement of dislocations and dislocation networks to mobile high angle grain boundaries and the migration of these, leading to a retardation of recrystallisation (Koster, 1971).

It has been suggested by Cahn (1965) that if the dispersion drag is insufficient, too much normal grain growth occurs, if the dispersion drag is too great, the secondary grains can-not grow at all. As shown in figure 2.8 the primary grain size of the pure alloy increases more rapidly than that of an alloy doped with a manganese-sulphide dispersion; the latter undergoes secondary recrystallisation, the former does not (Cahn, 1965).

A dramatic illustration of the importance of even very small amounts of dispersed phase in promoting secondary recrystallisation is provided by the work of Calvet and Renon (1960). They heat-treated a number of aluminium-copper solid solutions at a temperature close to the solid solubility limit. Effective inhibition of normal grain growth and very rapid secondary recrystallisation was observed, whenever the annealing temperature was as little as 1 to 2°C below the temperature at which all the copper present just entered into solid solution; at or above this temperature only rapid normal grain growth was observed. The dividing line between the two modes of recrystallisation in alloys of different compositions accurately traced out the known solubility curve. The volume fraction of dispersed phase just below the solubility line must be very small, less then 0.001%, but this is apparently enough to retard normal grain growth quite severely and thus permit secondary recrystallisation.

It is very well established that the second-phase particles may either stimulate or decelerate the recrystallisation process as compared with the behaviour of a single phase alloy (Humphreys, 1979). It has long been recognised by Doherty and Martin (1962), that the interparticle spacing is of particular importance in determining the recrystallisation kinetics. Alloys with large interparticle spacings show accelerated recrystallisation. The time for recrystallisation or the recrystallisation temperature is reduced as the particle size increases for a given volume fraction (Mould & Cotterill, 1967 and Hansen & Bay, 1972).

17

The number of recrystallisation nuclei formed at a particle, is also a function of the particle size (Humphreys, 1980a). Humphreys (1977) observed that for particles in the size range 1-5μm, usually only one grain is nucleated, but at particles larger than about 10μm, multiple nucleation is frequently observed by English and Backofen (1964), Herbst and Huber (1978), and Bay and Hansen (1979).

2.5 Grain Growth

The process of primary recrystallisation is generally considered to be complete when the boundaries of expanding, recrystallised, regions have migrated through the metal to such an extent that they have impinged on each other, thereby replacing the original deformed structure by a new strain-free polycrystalline structure. At this stage of annealing the metal has a new grain size which is the minimum that can be attained for the particular combination of metal composition, amount and form of prior deformation and annealing temperature. However, although the relatively high internal energy of the deformed state has been removed by primary recrystallisation, the resulting structure is in principle metastable and a further reduction in overall free energy can be achieved by a reduction of the total grain boundary area within the metal. Hence, a continuation of annealing leads to further migration of grain boundaries through the recrystallised structure, thereby a structure containing a smaller number of enlarged grains and this process of grain coarsening is known as grain growth (Cotterill and Mould, 1976).

In other words "the uniform coarsening of the grain structure of a stress-free material maintained at high temperature is described as grain growth". Grain growth is normally regarded as a process following primary recrystallisation but in principle it may also be observed in cast metals (Christian, 1965). According to Christian (1965) the driving force for this process, is the surface free energy of the boundaries remaining in the specimen. The driving force is proportional to $(1/r_1) + (1/r_2)$, where r_1 and r_2 are the two principal radii of curvature in mutually perpendicular directions of a local section of a boundary. Observations of boundary migrations on a planar section may be made by quenching the specimens at intervals during the growth, or by observing continuously with a hot stage microscope. Such observations show that boundaries generally migrate towards the centre of curvature, as required by the above assumption about the driving force. The requirements of local surface free energy at three grain junctions can be fairly readily met by relatively small atomic
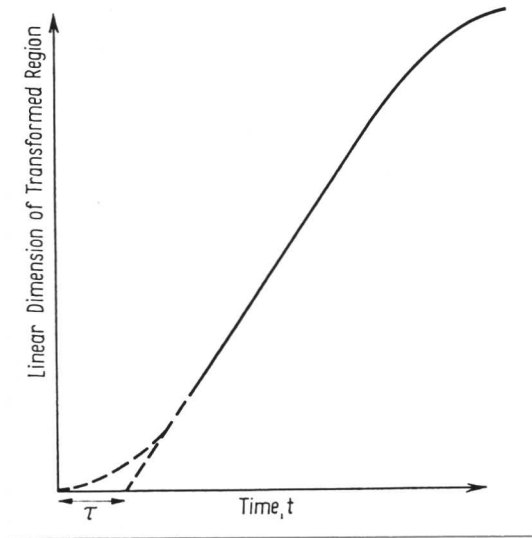
Figure 2.7. Schematic growth curve for a product region (after Christian, 1965).
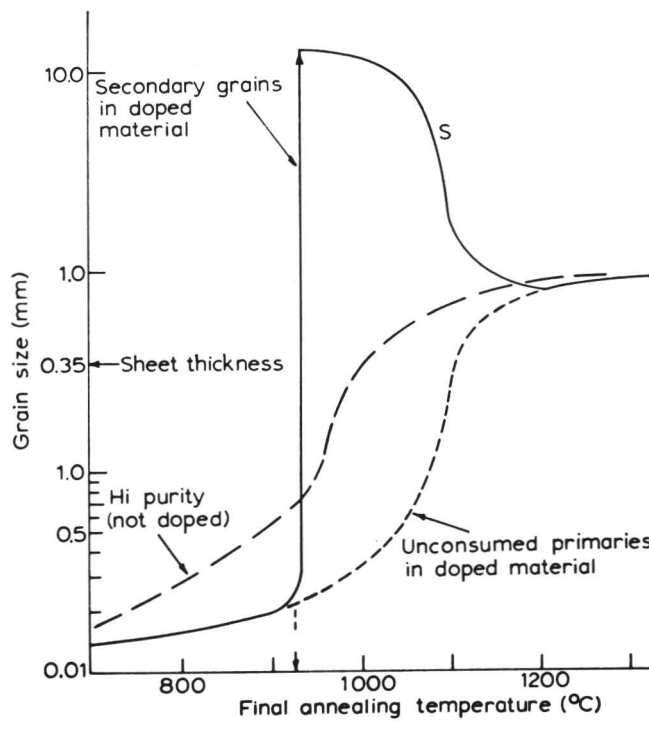
Figure 2.8. Grain size (log scale) as a function of temperature of pure and MnS-doped 3% Si-iron cold-rolled 50% to 3.5 mm thickness, and annealed 1 hour. The drop in the S curve is due to an increase in the number of secondary grains at high temperatures, until above 1100°C all grains grow equally to a size limited by the sheet thickness (after Cahn, 1965).

19

adjustments, so that under most conditions the angular relations of the three surfaces which meet at an edge will be maintained close to the equilibrium configuration. In order to satisfy this condition, most of the boundaries cannot be planar, and hence will migrate towards their centre of curvature by a process of atom transfer across the boundaries. This migration will generally be continuous, but occasionally unstable situations will arise leading to a rapid re-adjustment and corresponding discontinuities in the motion. Figure 2.9 shows how the migration of the boundaries towards the centre of curvature gives grain junction which immediately separates into two new three-grain junctions. In figure 2.9, growing grains A and C, each acquire a new surface as a result of this process, and shrinking grains B and D each lose a surface. By means of this type, grains occasionally increase or decrease the numbers of their bounding interfaces, and grains with only three interfaces are periodically eliminated completely. In principle, grain growth should continue until the whole specimen is a single crystal, or at least until the grains have dimensions comparable with the smallest external dimensions of the specimen, the grain boundaries then being planar and stable. This is sometimes observed but more usually a limiting grain size is achieved, after which grain growth virtually ceases. The blocking of grain boundary migration may be effected by inclusions (Christian, 1965).

Holmes and Winegard (1959-60), investigated the effects of small additions of lead, bismuth, silver and antimony on the grain growth of zone-refined tin. They found that the grain growth was retarded to an increasing extent in going from lead to bismuth to silver as solute. Rhines and Paterson (1982) investigated the effect of degree of prior cold-work on the rate of grain growth of recrystallised aluminium. They concluded that the range of grain size decreases monotonically with the degree of cold-work of the metal preceding recrystallisation. They also state that the rate of the grain growth decreases with increasing the degree of cold-work prior to recrystallisation.
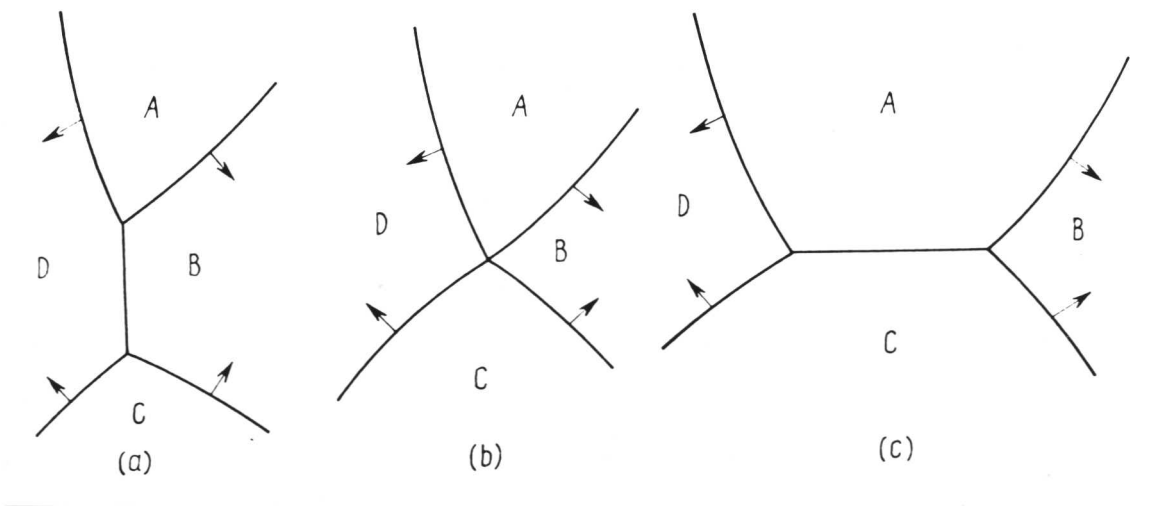
Figure 2.9. The migration of the grain boundaries in (a) produces the unstable four grain junction of (b) which immediately splits into two three-grain junctions (after Christian, 1965).

2.6 Rapidly Solidified Aluminium-Chromium-Zirconium Alloys

Low density aluminium alloys produced by rapid solidification technology have the potential to replace titanium alloys in aerospace applications, where service temperatures preclude the use of conventional aluminium alloys (Miller and Palmer, 1985). A number of applications have been identified (Thomas et al., 1986), for rapidly solidified Al-Cr-Zr alloys in aircraft structures, engines and in missiles, which can be summarised as follows:

Aircraft:

- general structure for high speed aircraft (>mach 2.5).

- engine support structure for all aircraft.

- exhaust shield supports.

- hot air ducting.

- wheels.

Engines:

- low temperature fan and compressor cases.

- blades and vanes.

Missiles:

- fins, winglets.

- skins.

- support structure.

The potential for these aluminium alloys has also been identified in industrial and automotive engines, in particular in piston and in connecting rods. The main advantage of rapidly solidified aluminium alloys over competitive materials are in the area of weight and cost savings. These results from the lower density of the alloys compared to titanium or steel, and the relatively low machining and fabrication costs (Thomas et al., 1986).

2.6.1 Production of Rapidly Solidified Aluminium Alloys

1. Solidification Techniques

The principal technique used commercially for the production of RS aluminium alloys is atomisation. There are wide variety of methods used to atomise aluminium alloys e.g., air atomisation, inert gas atomisation, centrifugal atomisation, and ultrasonic atomisation (Lawley, 1977).

2.6.2 Gas Atomisation Process

In gas atomisation, one or more high velocity air jets or other gas impinges upon a stream of molten metal. The molten metal stream is broken up into small particles, generally allowed to solidify in flight by convection and radiation (Lawley, 1977). The cooling rates depend strongly upon particle size, with higher rates as particle size decreases. There is a wide distribution in particles size, but generally quench rates in the range of 100 - 10,000°C / second are achievable (Maringer, 1980).

Production rates of tens of pounds per minute can be achieved, and the process can be adapted to batch or continuous operations. The powder handles and pours well. With aluminium, however, a special problem exists. When aluminium powders are handled in moist air, hydrates tend to form on their surfaces (Tietz & Palmer, 1981). These, if not removed, tend to form blisters on subsequent solution annealing. Thus, green compacts of aluminium are generally canned, evacuated and outgassed at some appropriate temperature (as high as 500°C) prior to consolidation by hot pressing, hot isostatic pressing, extrusion etc (Maringer, 1980). The general requirements of the atomisation process are:-

a. Molten Metal Treatment

To ensure the advantages of rapid solidification are obtained it is usually necessary to have melting furnace with a high temperature capability >1000°C. This is essential for alloys which contain transition metal additions such as Fe, Mo, V, Cr or Zr. For alloys intended for structural applications low gas levels are described and a high level of metal cleanliness is essential (Miller & Palmer, 1985).

b. Particle Size and Shape

The key feature of an atomising unit should be to produce a high yield of fine powder e.g., ideally around 50µm to 25µm in diameter to achieve structural uniformity. The shape of the particles depends on the atomising gas. Atomisation in the presence of oxygen produces an acicular powder. The shape of this powder can be an advantage since it aids consolidation due to interlocking between the powder particles (Ramaswamy & Ramakrishnan, 1981). In contrast inert gas atomisation produces a spherical powder, which is more difficult to consolidate.

The size distribution of the powder also influences subsequent consolidation. A wide range of particle sizes can be an advantage since the smaller particles fill the voids between the larger particles. However, a wide range in particle size implies a wide range in solidification rates and

hence in microstructure, which is likely to be detrimental to the final product (Miller & Palmer, 1985).

The other main technology for producing rapidly solidified (RS) aluminium alloys is substrate quenching e.g., melt spinning, melt drag, splat quenching and planar flow casting (PFC). The particulates so produced are generally in a form unsuitable for direct processing. Comparison of the consolidation behaviour of powder and flake has shown that flakes are more difficult to consolidate and are prone to delaminar failure (Paris et al., 1980). This is due to their tendency for a poor interfacial bonding between the individual flakes (Maringer, 1980). Consequently substrate quenched materials generally require processing to a finely divided form prior to consolidation. However, provided the process parameters are well controlled, techniques such as planar flow casting have the potential to produce a more uniform microstructure than atomisation.

2. Consolidation

Aluminium alloys have an oxide film on the surface, even after inert gas atomisation. This reacts with any moisture to form a hydrated oxide $Al_2O_3.3H_2O$. This hydrated oxide breaks down during processing to produce water, hydrogen and further oxide. The resulting gases can cause blistering and hydrogen embrittlement (Tietz & Palmer, 1981).

A number of techniques have been developed to degas the powder prior to consolidation (Kim et al., 1983). Generally they involve heating the partially consolidated material under a dynamic vacuum. From the metallurgical point of view the degassing time and temperature should be minimised to avoid the microstructural degradation. In the case of thermally stable alloys where processing and service temperatures are generally below 350-400°C, it may not be necessary to decompose monohydrate since this is stable at these temperatures (Pickens, 1981). The problem of degassing time, i.e., sufficient to remove degassing products but avoid structural degradation, will increase as billet size increases. The difficulty is in heating large masses of powder with poor thermal conductivity. For pellets in the size range 7-9 mm diameter, a degassing time of 6-8 hours is required. Techniques will have to be developed to satisfactorily degas large volumes of powder and this will probably involve dynamic methods, rather than the static ones currently in use.

The most general method of consolidation is extrusion and the main requirements for this method are:

1. Low temperature to avoid coarsening of the rapidly solidified microstructure.

24

2. An extrusion ratio of at least 15:1. This is necessary to fully disrupt the oxide film.

3. Minimisation of frictional heating during extrusion by appropriate die design. A typical production sequence is shown in figure 2.10 (Miller & Palmer, 1985).

2.6.3 Background of RS Al-Cr-Zr Alloys

The earliest use of powder metallurgy alloys in improving the high temperature of aluminium was the development of (SAP) sintered aluminium powders (Bloch, 1961). Early work in the United Kingdom (U.K.), showed that Al-8wt% Fe alloys were capable of achieving high strength and improved thermal stability (Thursfield and Stowell, 1974).

Initial work at Alcan (Marshall et al., 1986) assessed the influence of chromium and zirconium on thermal stability for a wider range of compositions. It was found that the alloy with the additions of chromium was resistant to solute clustering and precipitate coarsening at elevated temperatures (450°C), while maintaining a high degree of solid solution strengthening. In contrast, the additions of zirconium produced an age-hardening response. Figure 2.11 shows the influence of chromium and zirconium content on the microhardness of rapidly solidified particulate. It is clear that the age-hardening response is enhanced by increasing the zirconium content. However, the addition of chromium serves only to increase hardness without changing the extent of ageing response.

It was concluded by Marshall et al. (1986), that the alloys containing 4-5wt% Cr and 1.5-2wt% Zr provided a satisfactory basis for further development. The ageing response of a mid-composition range alloy is shown in figure 2.12 for a number of temperatures. A substantial ageing response is apparent at temperatures in the range of 350-450°C, with attainment of peak hardness after times varying from 1 to 24 hours. Moreover, the more significant features are the low hardness of the as-produced rapidly solidified particulate and the slow ageing response at normal working temperatures. These aspects aid the consolidation of rapidly solidified particulates into a wrought form which can then be heat treated to required level of strength and thermal stability. The composition of the alloy discussed is Al-4.82Cr-1.40Zr-1.41Mn wt% and is one of a series of alloys under development which also contain manganese additions, which significantly improve the thermal stability of Al-Cr-Zr alloys (Hughes et al., 1985).

25
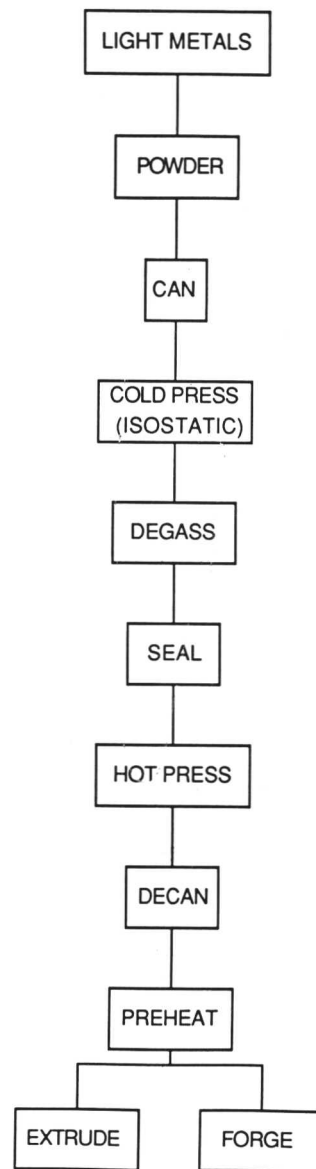
Figure 2.10. Typical production sequence for powder metallurgy (PM) ingot (after Miller and Palmer, 1985).
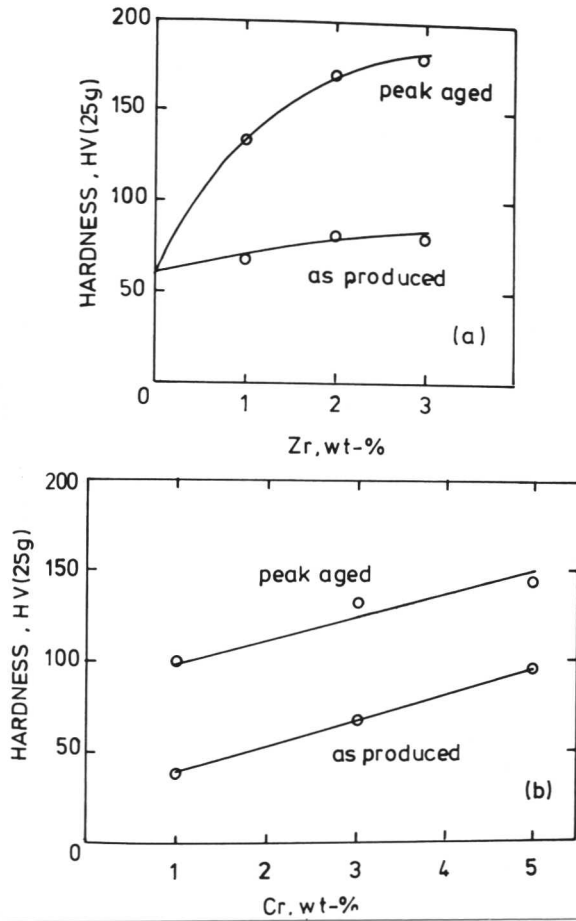
Figure 2.11. Influence of elemental additions on as-produced and peak-aged hardness of splat quenched Al alloys. (a) addition of Zr to Al-3wt% Cr. (b) addition of Cr to Al-1wt% Zr (after Marshall et al., 1986).
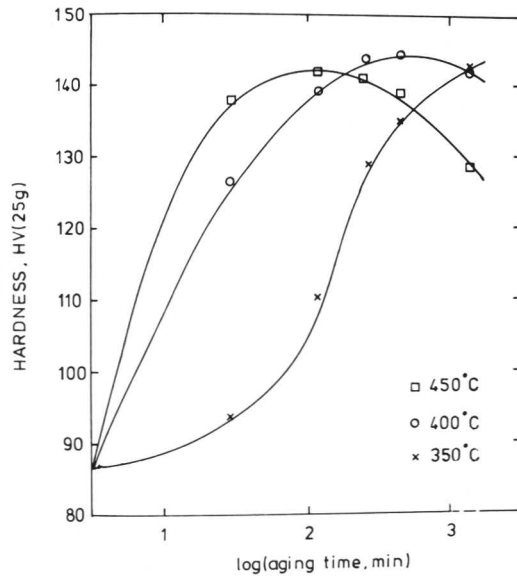
Figure 2.12. Influence of temperature on aging characteristic of Al-4.5Cr-1.7Zr (wt%) splat quenched alloy (after Marshall et al., 1986).

2.6.4 Physical Metallurgy of RS Aluminium Alloys

Thomas et al. (1986), examined the microstructure of the extruded material using transmission electron microscopy, and they noted the inhomogeneous nature of the microstructure. Some fine Al_3Zr dispersoids and also regions of the coarser $Al_{13}Cr_2$ phase were observed.

According to Thomas et al. (1986), ageing of the wrought material at 300°C for periods up to 1000 hours results in only a slight increase in the density and size of the Al_3Zr particles, consistent with the low diffusivity of zirconium in aluminium.

The broad $Al_{13}Cr_2$ peak observed in DSC (differential scanning calorimeter) trace from the hot compacted powder (figure 2.13), shows that in this condition chromium can begin to precipitate from solid solution or coarsen at temperatures below those anticipated from studies of as-atomised powder. The effect combined with hot working experienced during the extrusion process itself, can result in partial decomposition of the chromium solid solution in wrought material. The decomposition may result in coarsening of the dispersoid as well as the nucleation of new particles on dislocations. Satisfactory consolidation of the alloy powder is dependent, therefore, upon the thermomechanical cycle encountered prior to and during consolidation. Clearly the higher the extrusion temperature, the more important is the control over the prior thermomechanical treatment (Thomas et al., 1986).
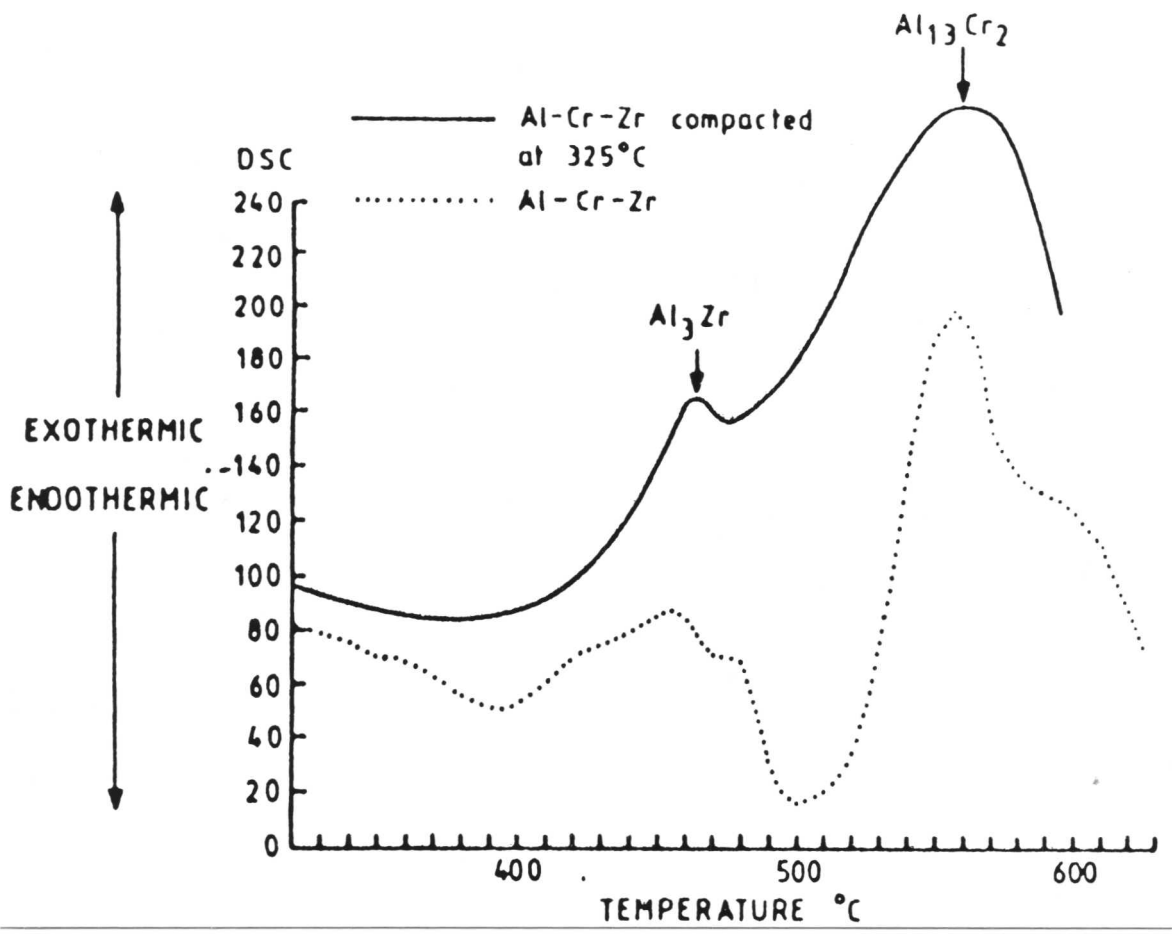
Figure 2.13. DSC (differential scanning calorimeter) traces from as-atomised powder and from powder compacted at 325°C (after Thomas et al., 1986).

2.7 The Development of Strong Alloys by Mechanical Alloying

The development of higher strength capability in metallic materials has generally been achieved by increasing the number and level of alloying additions. The sequential development of wrought iron, carbon steel, low alloy steels and highly alloyed steels is an obvious example, there are parallels in copper and aluminium alloys (Fleetwood, 1986). But perhaps the most celebrated sequence of alloy development is that of the nickel-base superalloys, and it was in seeking to raise their limits by another notch that mechanical alloying was developed (Hack, 1984).

Mechanical alloying originated from a long search for means to add high-temperature strength conferred by a fine dispersion of ceramic particles to the intermediate temperature strength developed by conventional alloying. According to Benjamin (1970), from the initial laboratory success in 1968, the process has been developed into a well-controlled production operation: whole series of nickel, iron, aluminium and other alloys have been designed specifically to use the process, and techniques have been developed to form and fabricate the alloys into useful components. After many years of development, mechanically alloyed (MA) materials are now in limited use in a range of applications, but work continues to extend their use (Fleetwood 1986).

2.7.1 The Mechanical Alloying Process

The mechanical alloying process is divided into two major parts: 1. high-energy milling; 2. consolidation and structure control.

1. High-Energy Milling

Mechanical alloying makes possible the combination of dispersion, solid-solution and precipitation strengthening by mechanical mixing all the constituents in powder form ever more intimately until diffusion completes the formation of true alloy powder (Gilman & Benjamin, 1983). Mixing is achieved by dry high-energy ball milling, under conditions such that the materials are not only fragmented but also rewelded together, a process prevented in conventional ball milling by the use of liquids and surfactants. Throughout the period in which mechanical alloying was being developed, high-energy milling was performed in attritors, in which the ball charge is stirred vigorously with rotating paddles (Fleetwood, 1986). The first commercial production used attritors which were able to process up to 34 kg of powder per charge, but in the latest production units, up to 1 ton of powder is processed in 2 m diameter mills containing more than a million balls which weigh a total of around 10 tons. The charge is a blend of elemental and prealloyed powders, at least

one of which is a ductile material, and a crushed master alloy containing intermetallic compounds of the most reactive elements. For example, titanium and aluminium are added as Ni-Ti-Al alloy, which has a much lower activity than pure titanium and aluminium. To provide a dispersed phase in nickel and iron base alloys, fine inert oxides such as Y_2O_3(yttria) can be included into the charge. Weber (1980), illustrated the effect of a single high energy collision between two balls on powder trapped between them (figure 2.14). The ductile elemental powders are flattened, and where they overlap, the atomically clean surfaces just created weld together, building up layers of composite powders and the dispersoid. At the same time work-hardened elemental or composite powder fracture. These competing processes of cold welding and fracture occur repeatedly through out the milling, gradually kneading the composites so that their structure is continually refined and homogenised. After the initial stage of milling the composite shows coarse layers of identifiable starting materials, with the dispersoid closely spaced along the welds. After more refinement through fracture and welding, the composites develop a structure of convoluted lamellae of decreasing thickness between welded surfaces along which dispersoids are closely spaced. The combination of severe cold-work and heating from the kinetic energy of balls aids diffusion and as diffusion distances continually decrease by the finer mixing of constituents, solute elements dissolve, areas of solid solution grow in composite powders and metastable phases may precipitate. In the final stage of milling the lamellae become more convoluted and thinner ($< 1\mu m$) and the composition of individual particles converges to the overall composition of the starting powder blend. Precipitation of equilibrium phases occurs, work hardening and softening reaches a balance, and the microhardness of the individual powder particles attains a saturation value around 650 kg mm^{-2} for Fe-Cr alloys (Gilman & Benjamin, 1983). Finally the lamellae are no longer resolvable optically and the distance between dispersoid particles along the weld interfaces, approximately equal to the spacing between the welds. Then, the composition of individual powder particles is equivalent to that of the starting blend and mechanical alloying is complete. Further milling will produce no further homogenisation in either the matrix or the dispersion (Fleetwood, 1986).

2. Consolidation and Structure Control

Oxide dispersion strengthened powders do not densify on simple sintering and the high hardness of mechanically alloyed powder prevents cold pressing, so the powder discharged from the mill must be consolidated by a combination of high temperature and pressure, hot compaction plus hot extrusion in a can, or hot isostatic pressing (Gessinger, 1984). Extrusion of canned powder is
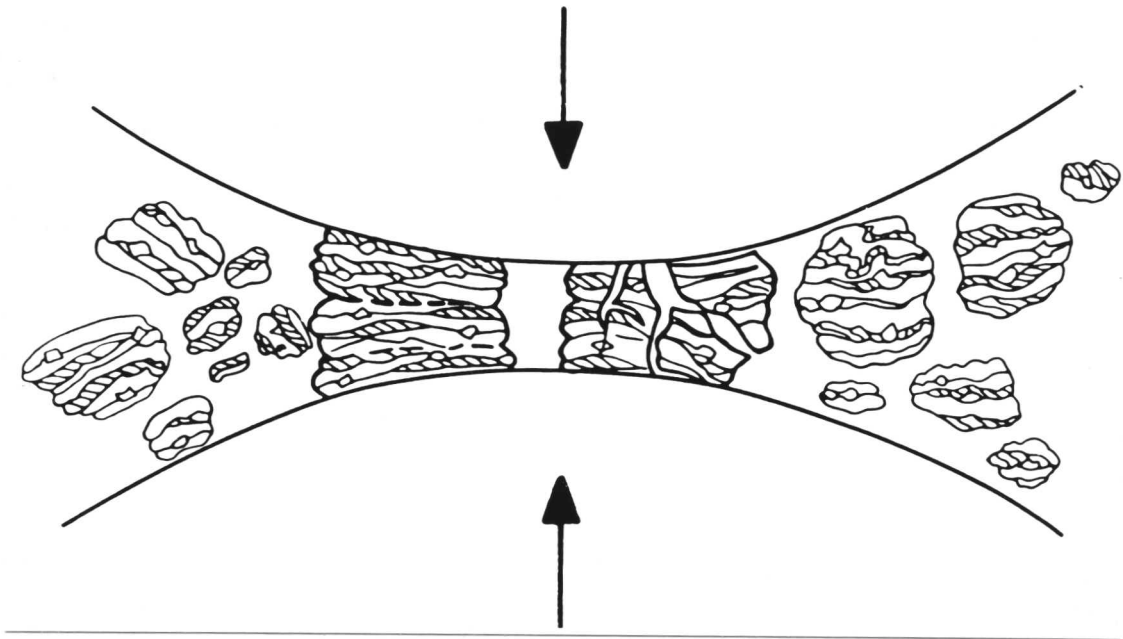
Figure 2.14. Schematic diagram showing the effect of single collision between two balls on trapped powder (after Weber, 1980).

generally preferred, being the cheapest process and able to provide anisotropic structures with good properties (Fleetwood, 1986). High temperature treatment before hot consolidation completes homogenisation by diffusion. Any further processing after extrusion must be carefully controlled to generate the optimum grain structure for particular applications. Two microstructures are beneficial:

1. Fine equiaxed grains, giving the best room temperature strength, fatigue strength and workability.

2. Coarse elongated grains, giving the best room temperature stress-rupture strength and thermal fatigue resistance. The fine grained condition exists in extruded material, whereas coarse elongated grains are developed by recrystallisation of material thermomechanically processed to produce a high level of stored strain energy. It is a complex matter to control the stored energy, which depends on the whole thermomechanical processing history of the material: from the conditions of milling, through the temperature, ratio and speed of extrusion, to the details of post extrusion processing, including hot and cold rolling or forging, and the grain coarsening anneal. Achievement of the highest strength attainable by mechanically alloyed material demands the closest control of production (Fleetwood, 1986).

2.7.2 Processing and Properties of Inconel Alloy MA6000

Nickel is charged to the ball mill as 4-7μm elemental powder, chromium, molybdenum, tungsten and tantalum as ~150μm elemental powder and the most reactive elements aluminium, titanium, boron and zirconium ~150μm crushed nickel-base master alloys. Y_2O_3 is added as 1μm agglomerates of 20-40 nm particles, on completion of mechanical alloying, the dispersoid is a mixed oxide of Y_2O_3- Al_2O_3.

To optimise the properties the recrystallised alloy is heat treated for 0.5 hour at 1230°C and air cooled to take γ' into solution and for 2 hours at 955°C air cooled + 24 hours at 845°C and air cooled to precipitate the γ' of the best size and distribution. Figure 2.15 compares the specific rupture strengths (strength/density) for 1000 hours life as a function of temperature for MA6000 and other high strength alloys. MA6000 approaches directionally solidified nickel base superalloy DS MAR-M200+HF in strength and is progressively stronger than the cast alloys at temperatures above about 900 °C, as γ' strengthening declines (Fleetwood, 1986).
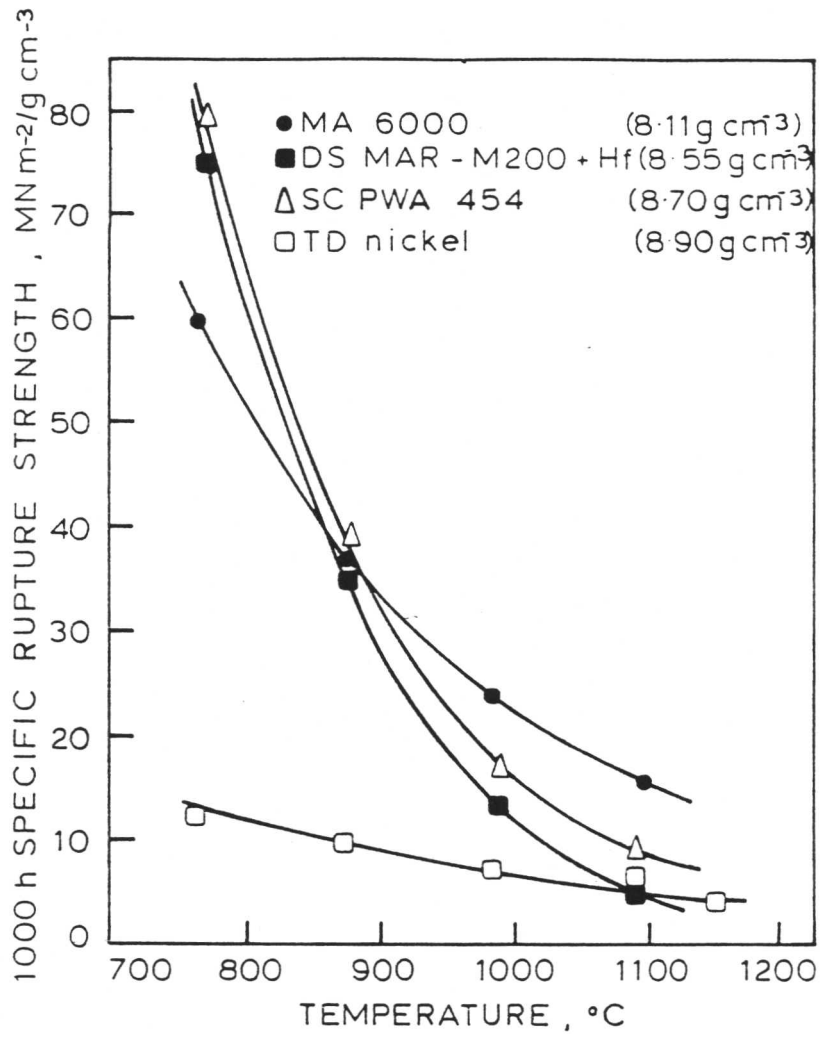
Figure 2.15. Specific stress-rupture strength for 1000 hours of Inconel MA6000 compared with other high-strength alloys (after Fleetwood, 1986).

2.7.3 Oxide Dispersion Strengthened Ferritic Alloys

Recently, advanced ferritic-base oxide dispersion strengthened alloys have been developed. The most highly developed material is Incoloy alloy MA956 (Fe-20Cr-4.5Al-0.4Ti wt%) and is dispersion strengthened with Y_2O_3. MA956 has been made in the form of bars, sheets, plates, wires, tubing, forgings, rings, hot spinnings and fabrications.

2.7.4 Production and Properties of Incoloy Alloy MA956

MA956 is mechanically alloyed from elemental iron powder, Fe Cr Al Ti master alloy crushed to ~150μm, and Y_2O_3 powder is added and hot compacted by extrusion. Bar stock is made by extrusion and hot rolling followed by static annealing to attain the recrystallised grain structure, elongated along the rolling direction. Plates and sheets require hot and cold rolling, with hot cross-rolling to obtain "pancake" shaped grains after recrystallisation giving isotropic properties in the plane of the sheet. The first step of tube making is hot compaction by direct upsetting against a die in the extrusion press to provide a 300 mm diameter billet. This is bored to a hollow perform, conventionally extruded to a tube shell, and then this tube reduced on a Pilger mill. The resulting fine grained tube is recrystallised to coarse grains elongated along the tube axis (Fleetwood, 1986).

MA956 in the form of bar and sheet exhibits high stress rupture strength. The high strength capability is combined with exceptional high temperature oxidation and corrosion resistance, associated with the formation of alumina oxide scale (Kane et al., 1984). MA956 has a good cyclic oxidation resistance. The alumina scale is an excellent barrier to carbon in situations where carburisation occurs in hydrogen methane mixture at 1000°C. Sulphidation resistance is also good (Fleetwood, 1986).

2.7.5 Fabrication and Applications of MA956

MA956 cold rolled annealed sheet is readily formed into complex components. However, because the alloy behaves as a ferritic steel, it has reduced ductility during forming below its ductile-brittle transition temperature, which is 0-80°C, dependent on product form and stress rate (Incomap). Although the forming of simple shapes is possible at room temperature, more complex operations are best observed by slightly warming the material to 100°C (Robinson, 1982). This material can be formed in hot finished or fine grained condition. Both hot spinning and ring rolling are used to manufacture components having circular symmetry. After forming, the fine grain components are annealed at 1300-1350°C to produce normal coarse recrystallised grain structures (Hack, 1984).

MA956 may be tungsten inert gas welded using a near matching Fe-Cr-Al filler wire for corrosion resistance but such welds have less strength at high temperatures, than the wrought sheet alloy. Electron beam and laser welds have been shown to have useful high temperature properties, as high brazed joints (Hack, 1984). Riveting using MA956 rivet rod, has also been effective in several applications (Macdonald, 1981). The forging of the mechanically alloyed oxide dispersion strengthened is normally carried out with work piece in a fine grain condition, i.e., as-rolled or as-extruded. No problems are experienced in forging MA956, using conventional techniques (Hack, 1984).

The sheets, plates, spinnings, rings and forgings of MA956 have applications in combustion chamber and turbine casing sections where the resistance of the alloy to creep, oxidation and sulphidation allows higher metal temperatures and longer component life. The relative ease with which the ferritic Incoloy alloy MA956 may be hot and cold-worked has made possible a wide range of mill forms suitable for general industrial applications requiring temperatures up to 1300°C (Hack, 1984).

One of the non-aerospace applications of MA956 is for burner hardware in coal and oil burning power stations. The burner flame stabliser, made from MA956 sheet and rivets, is used for in severely corrosive environment in which metal temperatures up to 1230°C are experienced (Macdonald, 1981). The use of this alloy allows several thousand hours of operation without any distortion or significant wastage. MA956 is also used in fluidised bed combustion and has been evaluated successfully for local gasification in which the resistance to sulphidation and carburisation is outstanding (Lloyd and Cooke, 1981).

CHAPTER THREE

Experimental Techniques

3.1 Materials

As mentioned earlier, in order to obtain a high level of confidence in any attempt at modelling the directional recrystallisation, it was essential to cover a wide range of temperatures and time. For this reason experiments have been conducted on a variety of materials, including oxide dispersion strengthened alloys and aluminium alloys. The chemical compositions of the materials used are given in Table 3.1.

Table 3.1. Chemical compositions of the materials investigated.

Alloy designation	Chemical Composition (wt%)										
	C	Cr	Al	Ti	Ta	Mo	W	Zr	B	Y_2O_3	Balance
MA6000	0.05	15	4.5	2.5	2	2	4	0.15	0.01	1.1	Ni
MA956	0.01	20	4.5	0.5	—	—	—	—	—	0.5	Fe
MA957	0.01	14	~~10~~	1.0	—	0.3	—	—	—	0.27	Fe

Alloy designation	Chemical Composition (wt%)						
	Cr	Zr	Mn	Mg	Si	Fe	Cu	Balance
Al5	4.82	1.40	1.41	—	—	—	—	Al (Air atomised)
Al15	5.20	1.89	0.96	—	—	—	—	Al (Nitrogen atomised)
AA3003	—	0.1	1.2	—	0.6	0.7	0.1	Al
Al20	—	0.1	—	0.95	0.8	0.7	1.25	Al (20wt%SiC reinforcement)

3.2 The Fabrication Details

Mechanically alloyed oxide dispersion strengthened alloys and low density aluminium alloys produced by rapid solidification technology and commercial aluminium alloys have been used to study the directional recrystallisation. The processes involved in mechanical alloying and rapid solidification technology are discussed in detail in chapter 2. In this section the fabrication details of the specific alloys used in the present work are described.

Inconel[*]MA6000

Inconel MA6000 is an oxide dispersion strengthened nickel base superalloy. The mechanically alloyed MA6000 was fabricated by charging nickel to the ball mill as 4 - 7 μm elemental powder, chromium, molybdenum, tungstun and tantalum as -150 μm elemental powders, and the most reactive elements aluminium, titanium, boron and zirconium as -150 μm chrushed nickel base master alloys. Y_2O_3 is added as 1 μm agglomerates of 20 - 40 nm particles (Incomap).

Consolidation was achieved by extrusion of the powder in a mild steel can. The extruded size for Inconel alloy MA6000 was 54 mm diameter. Alloy was rolled with the can in-situ. Conventional hot rod rolling methods were used to process the extruded bar, the hot-rolling temperature was 1040°C. Inconel alloy MA6000 bar was subsequently decanned by acid pickling (McColvin, 1987). The material was supplied in the hot-rolled condition with the dimensions of 20 mm diameter and 800 mm long, with no subsequent heat treatment applied.

Incoloy[*]MA956 and MA957

Incoloy MA956 and MA957 are oxide dispersion strengthened ferritic stainless steels. ODS ferritic steel MA956 was fabricated by charging three primary powders, elemental iron, a pre-alloyed chromium rich master alloy and yttria, to a water cooled vertical attritor and milled (Incomap).

The consolidation of the resultant powder was achieved by extrusion of the powder in a mild steel can, for the Incoloy alloy MA956 the extruded size was 65 mm diameter. The alloy was then machined to remove the mild steel can prior to rolling. Conventional hot rod rolling methods were used to process the extruded bar. The extruded bar of Incoloy MA956 has been hot-rolled at 1000°C (Incomap). The Inconel alloy MA956 bar was the representative sample of the commercial grade material and Inconel alloy MA957 was taken from a development program, no further information about the fabrication details for MA957 has been given by the suppliers. Both bars were

received in the hot-rolled condition with no subsequent heat treatment applied, with the dimensions as follows:

1. Inconel alloy MA956 hot-rolled bar 25 mm diameter ×1000 mm long.

2. Inconel alloy MA957 hot-rolled bar 9.5 mm diameter ×1000 mm long.

* Alloy names marked with an asterisk are all trade names of the Inco family of companies.

RST Al-5 (air-atomised) and Al-15 (nitrogen-atomised)

Rapidly solidified Al-Cr-Zr alloy powders were produced by the horizontal air atomisation and horizontal nitrogen atomisation methods (the atomisation process is described in detail in chapter 2). Each atomisation batch was sieved prior to consolidation, in order to remove coarser dispersoids as much as practically possible because the coarser $Al_{13}Cr_2$ if retained in a wrought product may act as crack initiation sites and therefore, degrade the mechanical properties of final product (Palmer, 1988).

Consolidation utilised the cold compaction of approximately 1 kg of powder to produce billets of 85% density which were then preheated for extrusion at 400°C. An extrusion ratio 15:1 was used to produce 19.1 mm diameter rod and all extruded bar was water quenched upon exit from the press (Marshall, 1989).

AA3003

The Al-Mn alloy (AA3003) was supplied by a commercial sheet ingot and hot rolled route. After hot rolling to 25 mm and slow cooling to room temperature, the slab was then cold rolled to 3.5 mm on a laboratory mill to give an 86% cold reduction (Marshall, 1989).

Al20

The alloy Al20 was supplied by British Petroleum. The nominal chemical composition for alloy Al20 is given in Table 3.1. The 20wt% SiC particles have been used for reinforcement. The SiC particles had an angular morphology (Knowles, 1989). The powder blending route commonly used to produce MMCs is shown in figure 3.1. The term MMC refers to a broad family of metal based materials reinforced with either fiber, whiskers or particulate to provide enhanced combination of properties (White et al., 1987). The matrix can be any metal or alloy, but most interest is being shown in structural applications where light weight and stiffness are required, thus the matrices are

usually aluminium, magnesium or titanium (Willis, 1988).

The fabrication process of alloy Al20, involved blending pre-alloyed powder with a SiC particulate reinforcement, followed by canning, vacuum degassing at 545°C for 24 hours, and consolidated by hot isostatically pressing (HIP) to 100% density at 540°C. After consolidation the aluminium can is removed by machining and the material extruded. The extruded bar of alloy Al20 was received with the dimensions of 15 mm diameter and 1000 mm long.

3.3 Zone Annealing

Zone annealing was carried out using a crystal grower as the way of achieving directional recrystallisation. The specimens were placed in a silica tube, mounted on a carriage driven by a variable speed electric motor. A Pt/Pt-13wt%Rh thermocouple was used to measure the temperature during operation, with one end of the thermocouple in the middle of the specimen and the other end attached to a Comark (a device which converts electrical potential to temperature) for measuring the temperature during the movement of the specimen through the R. F. coil. The zone annealing experiments were performed in air. A schematic diagram of the crystal grower adapted and used is shown in figure 3.2.

3.4 Optical Microscopy

Optical microscopy was used to observe recrystallisation after different heat treatments. The specimens from aluminium alloys were cold mounted in resin to avoid unnecessary heating. The specimens were then ground on silicon carbide paper to a sufficient depth to remove any unrepresentative surface. After mechanically grinding down to 1200 grade emery paper, they were finally polished on a "Mastertex" final polishing cloth, using a colloidal silica polishing suspension.

Specimens from ODS alloys, after each successive heat treatment, were hot mounted using an automatic mounting press, and then mechanically ground down to 1200 grade silicon carbide paper and mechanically polished using 1μm diamond paste and finally polished on a "Vibromet" in a suspension of 0.5μm alumina powder in ethandiol.

A list of etchants used for the different materials is given below,

Material	Etchant
1. MA6000	2g $CuCl_2$, 40ml HCl, 40 to 80ml ethanol
2. MA956	2g $CuCl_2$, 40ml HCl, 40 to 80ml ethanol

3. MA957	2g $CuCl_2$, 40ml HCl, 40 to 80ml ethanol
4. Al-5	60%HF + 40%H_2O
5. Al-15	60%HF + 40%H_2O
6. AA3003	190ml Distilled water, 5ml HNO_3, 3ml HCl, 2ml HF
7. Al-20SiC	190ml Distilled water, 5ml HNO_3, 3ml HCl, 2ml HF.

Photography was carried out using an Olympus camera fitted to an Olympus light microscope.

3.5 Transmission electron microscopy

A Philips EM 400 T electron microscope was used for the examination of thin foils. The operating voltage was 120 kV. Thin foil specimens were prepared for transmission electron microscopy from 0.25mm thick discs slit from rapidly solidified aluminium alloys Al-5 and Al-15 in the as-received condition and after cold-working. The discs were thinned down to 0.05mm by abrasion on silicon carbide paper and then electropolished using a twin jet electropolisher. The polishing solution was a mixture of 10% perchloric acid in methanol at room temperature, at an applied voltage of 12 to 20V. Considerable difficulty was experienced in electropolishing, which may either be attributed to the polishing solution, or to the voltage applied, or most likely to the tendency for particles to fall out during electropolishing.

Transmission electron microscopy was also performed on ODS alloys, in the as-received condition and after each successive heat treatment in order to investigate the recrystallisation behaviour in these alloys. The thin foils were cut in a direction parallel to the directionally recrystallised grain structure from the samples zone annealed at different peak temperatures (T_p) and a variety of specimen travel speeds ranging from 0.2 to 10.0 mm/min. Thin foils were subsequently ground down to 0.05mm by abrasion on 1200 grit paper and then electropolished using twin jet electropolisher at room temperature. The polishing solution consisted of 20 vol% perchloric acid in ethanol in between 25 to 30 volts.

Particular attention has been paid to the study of orientation relationships between the directionally recrystallised grains, although it was often difficult to produce sufficient thin area near a grain boundary.

The axis-angle pair (i.e., orientation relationship) for two adjacent grains (discussed in chapter 4) were calculated using a computer program (Yang and Bhadeshia, 1989). The program requires the input of the components (hkl) of the any two vectors from crystal A and the components (hkl) of

the any two vectors of crystal B and the acute angle between vectors 2A of crystal A and 1B of crystal B. The program then calculates the rotation axis, right-handed rotation angle and finally gives the 23 equivalent axis-angle pairs.

3.6 Hardness Tests

The hardness tests were carried out using a Vickers hardness testing machine. Measurements were made on polished specimens. The indentation load applied was 10kg, otherwise as mentioned in the tables illustrating hardness results. All the measurements were made at a suitable distance from the specimen edge, in order to avoid any edge effects. At least five readings were taken per specimen.

3.7 Differential Thermal Analysis

Differential thermal analysis (commonly abbreviated to DTA) is a technique of recording the difference in temperature between a substance and a reference material as the two specimens are subjected to identical temperature regimes in an environment heated or cooled at a controlled rate. The record obtained is called the differential thermal or DTA curve and, provided the substance is thermally active in the temperature range used, shows a series of peaks, the position of which are determined by the chemical composition and crystal structure of the substance and the area of which (peak) is related to the energy involved in the reaction occuring (Mackenzie, 1970).

The area under a DTA peak can be directly and quantitatively related to the enthalpy changes involved, and is not affected by the heat capacity of the sample concerned (Bhadeshia, 1983).

The DTA experiments have been performed with the help of ESAB AB of Sweden, on a high THERMOVAG STA429 DTA apparatus. Samples of required dimensions (4mm diameter $\times$15mm long) were used. They used K_2SO_4 as a reference for all the experiments, because the data for the reaction occur in K_2SO_4, is easily available in the literature. The heating rate and the weight of samples and references used for differential thermal analysis experiments are listed in Table 3.2.

41

Table 3.2. Heating rate and weight of samples used for DTA experiments.

| Material	Heating Rate	Weight of Sample	Weight of Reference
MA6000	5 K/min	1.537 mg	100 mg
MA956	5 K/min	1.303 mg	50 mg
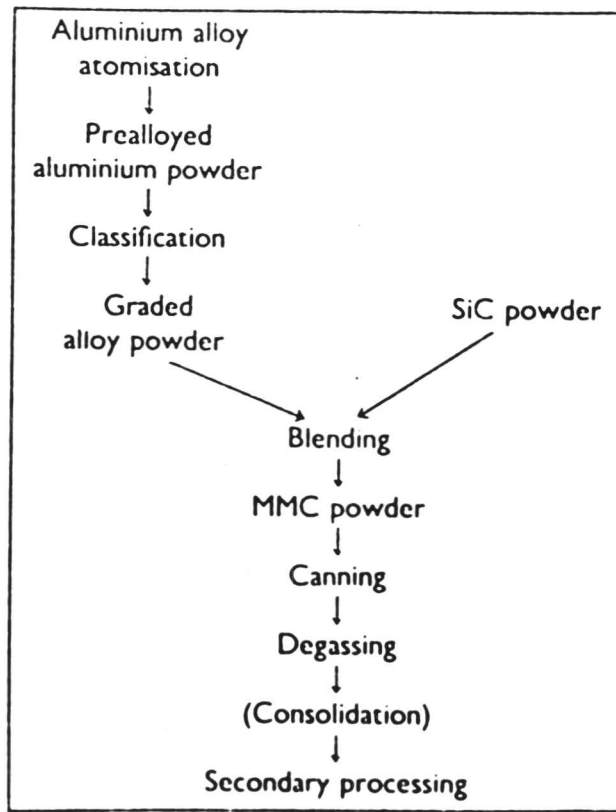
Figure 3.1. Flow sheet diagram illustrating the powder blending route commonly used to produce MMCs (after White et al. 1987).
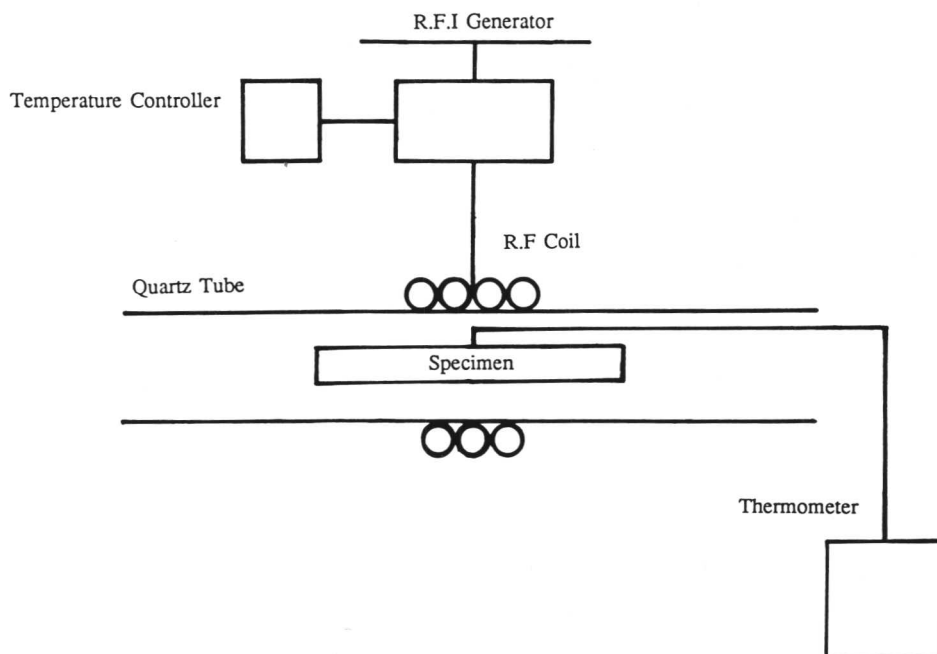

Figure 3.2. Schematic diagram of the crystal grower, used for zone annealing experiments.

CHAPTER FOUR

Characterisation of As-Deformed Microstructure of ODS Nickel Base Superalloy (MA6000) and ODS Ferritic Steel MA956

4.1 Introduction

Since the materials studied are unusual in the sense that they have been prepared from mechanically alloyed procedures (as explained in detail, in chapter 3), including compaction and "hot" extrusion, it was felt necessary to characterise the initial microstructure thoroughly prior to zone annealing experiments.

Following consolidation by "hot" extrusion, dispersion strengthened superalloys appear to display a very fine sub-micron grain size, consisting of both dislocation-free recrystallised material and unrecrystallised regions of high dislocation density. The grain size and dislocation density are related to thermomechanical processing parameters like strain, strain rate and temperature (Benn et al., 1984).

This chapter deals with an attempt at the characterisation of the as-deformed microstructure of two of the alloys used to study directional recrystallisation. The microstructural investigations and crystallographic studies have been carried out using the transmission electron microscope.

4.2 Transmission Electron Microscopy of As-Deformed MA6000

The thin foils examined using a transmission electron microscope, were for the oxide dispersion strengthened nickel base superalloy MA6000, prepared from the as-received hot-rolled bar of Inconel alloy MA6000. Since the deformed material had been given an 54% reduction in area had a hardness of 645 HVN(10kg), considerable efforts were required to prepare the thin foils. The microstructure examined from both transverse and longitudinal (with respect to the extrusion direction) sections of the as-received material is shown in figure 4.1.

Equiaxed grains, (figure 4.1) with an incredibly small grain size (Mean linear intercept[1] $\bar{L}$ = 0.174μm) were observed in both the transverse and longitudinal directions, with a very low dislocation density within the body of the grains. On further examination of the thin foils (figure

---

[1] The mean linear intercept $\bar{L}$ = L / N, where N is the number of grains counted in a defined length L.

4.2) annealing twins and subgrain boundaries (figure 4.3) were also observed.

These observations are not at all characteristic of a deformed sample. The equiaxed grain shapes are not expected in the longitudinal sections, and it is often the case that deformed samples exhibit anisotropic grains even in the transverse section. Straight annealing twins and uncluttered subgrain boundaries are also not consistent with an as-deformed microstructure. These observations, and the ultrafine grain structure indicate that the deformation conditions have caused the microstructure to undergo primary recrystallisation. Alternatively, the microstructure could simply reflect dynamic recovery, with the fine grains really corresponding to subgrains with low relative misorientations. A crystallographic investigation was therefore undertaken to distinguish between these possibilities.

4.2.1 Orientation Relationships between adjacent Crystals of ODS MA6000

To resolve the ambiguities made earlier, and to confirm that the nickel base superalloy MA6000 underwent a process of primary recrystallisation during hot extrusion, the orientation relationships between the adjacent grains of the as-received sample were investigated.

The results of 26 experiments are listed in Table 4.2. Five examples are illustrated as follows. Figure 4.4 shows the electron micrograph and corresponding convergent beam diffraction patterns (CBDP) from two adjacent grains of ODS alloy MA6000 in the as-received condition, grains A and B. The CBDP illustrates that grains A and B have the same zone axis <0 0 1>. The orientation can be represented by a rotation of 180° about <0.000 0.608 0.793>, an axis-angle pair determined from the diffraction patterns using a computer program (after Yang and Bhadeshia, 1989) on practical crystallography. The axis-angle pair on their own are enough to establish that the misorientations between the grains are far too large to be associated with the fine grained microstructure being generated by recovery (i.e., subgrain coalescence). A way of making the results more easy to appreciate, becomes apparent from the fact that subgrain boundaries are close to $\Sigma=1$ orientation. Thus, any higher Σ values indicate much larger orientations. Note that for cubic lattices, the orientation relationship between two grains can, as consequence of symmetry, be represented in 24 equivalent ways. By convention, it is the axis-angle pair with the highest angle of misorientation that is chosen to state the orientation relationship. The initial requirements for the calculation of axis-angle pairs, have been defined in chapter 3. From the values obtained for axis-angle pairs it is possible to estimate the nearest reciprocal density of coincidence sites (usually described as Σ values) between the two grain boundaries by converting the decimal values of the components of

the rotation axis into integers. The integers obtained from the axis-angle pair values are then matched with Table 4.1 given by Bhadeshia (1987), illustrating some of the coincidence site lattice (CSL) relations for cubic crystals. All of the CSL relations given in Table 4.1 can be represented by a rotation of 180° about some rational axis which is not an even axis of symmetry (Bhadeshia, 1987).

Aust and Rutter (1959) and Kronberg and Wilson (1949), described the coincidence site lattice by allowing the two lattices (with a common origin) are notionally allowed to interpenetrate and fill all space. There may then exist lattice points (other than the origin) which are common to both crystals. The set of these coincidence points forms a coincidence site lattice, and the fraction of lattice points which are also coincidence sites is a rational fraction $1/\Sigma$. Σ is thus reciprocal density of coincidence sites relatively to ordinary lattice sites (see for example, Bhadeshia, 1987). The approximate Σ value obtained for grains A and B was near $\Sigma 3$, the conventional twin orientation relationship.

Figure 4.5 shows that grains C and D have approximately the same zone axis <0 1 1>. The axis-angle pair relating to these grains can also be represented equivalently by a rotation of 180° around <0.372 0.656 0.656> and thus is near a $\Sigma 9$ orientation relationship. Figure 4.6 shows that grains E and F have approximately the same zone axis <0 0 1> as well. The axis-angle pair relating these grains can equivalently be demonstrated by a rotation of 160° around <0.618 -0.695 0.360> and this is not for from a $\Sigma 9$ orientation relationship. Figure 4.7 shows that the grains G and H of nickel base superalloy MA6000 in the as-received condition, have about the same zone axis <0 0 1>, the axis-angle pair associated with these grains can also be represented by <0.553 0.622 0.553> around 180°, which corresponds roughly to the value of $\Sigma 3$. Figure 4.8 shows grains I and J, axis-angle pair for these grains can also be represented as <0.650 0.322 0.687>/154°, and this is near a $\Sigma 9$ orientation relationship.

The convergent beam diffraction pattern (Figure 4.8c) which corresponds to grain J in figure 4.8a, clearly shows the superlattice reflections. The major phases present in the structure of nickel base superalloys are f.c.c austenite, γ, the matrix of the alloys and gamma prime γ', as the major precipitate phase (Decker and Sims, 1972, and Ricks et al. 1983, and Sims, 1984). The composition of γ' phase is usually considered to be $Ni_3(Al-Ti)$, and is described as a superlattice, possessing Cu_3Au ($L1_2$)-type structure by Stoloff (1972).

In the nickel base superalloy $Ni_3(Al\text{-}Ti)$, the γ' phase, is generally considered to be the major source of high creep resistance (Decker and Freemen, 1960). Nembach et al. (1988), have described that the nickel base superalloys are strengthened by coherent precipitates of the γ' phase, which has the ordered $L1_2$-type crystal structure.

From the examples given for the experimentally determined axis-angle pairs, and from other examples presented in Table 4.2, it is evident that the oxide dispersion strengthened nickel base superalloy (MA6000), contains randomly distributed high misorientation grain boundaries in the as-received condition, establishing that the ultrafine grained microstructure develops as a consequence of primary recrystallisation rather than recovery.

In the light of metallography and crystallographic results it can be said that alloy MA6000 was in the as-received, extruded condition in a recrystallised condition. Further annealing should therefore be considered to lead to secondary recrystallisation in which the ultrafine grains of the initial microstructure give way eventually to a very coarse grained microstructure.

4.3 Transmission Electron Microscopy of As-Deformed ODS Ferritic Steel MA956

Thin foils of alloy MA956 for transmission electron microscopy were prepared from the as-received hot-rolled bar. In that condition the material sustained an 54% reduction in area and had a hardness value of 350 HVN(10kg).

Figure 4.9 reveals the microstructure of the as-deformed alloy MA956, and appears to be heavily dislocated. From figure 4.9a, which was recorded during the examination of the thin foil prepared from the transverse section of the bar, an equiaxed grain structure (consistent with the circular section of the extruded bar) can be seen, containing a relatively high dislocation density. By contrast, longitudinal sections revealed an elongated grain structure, with tangled dislocation networks. Note that the longitudinal section contains rolling direction (figure 4.9b). The grain size, as measured by the mean linear intercept method from electron micrograph was found to be 0.45μm.

4.3.1 Orientation Relationship between the Adjacent Grains of ODS Ferritic Steel MA956

A total of twenty four experiments were performed to determine the orientation relationships between adjacent crystals of ODS ferritic steel MA956 in the as-received condition. The results obtained are listed in Table 4.3. Four examples are illustrated as follows.

Figure 4.10 shows an electron micrograph and corresponding selected area diffraction patterns (SADP) from two adjacent grains of ODS ferritic steel MA956 in the as-received condition. The

SADP clearly display that grains A and B have the same zone axis <1 3 3>. The axis-angle pair relating to these grains can also be represented, equivalently, by a rotation of 180° around <0.177 0.655 0.724>, and this is near a Σ13b orientation relationship. Figure 4.11 shows an electron micrograph and corresponding SADP's from a pair of ferrite grains, C and D. The selected area diffraction patterns (Figs. 4.11b & c) reveal that grains share the same zone axis <0 2 3>, and the orientation relationship can be equivalently described by a rotation of 180° around <0.205 0.814 0.542>, and this is again near a Σ13b orientation relationship. Figure 4.12 shows the electron micrograph and the corresponding SADP from another pair of ferrite grains E and F. The interface boundary between grains E and F is clearly displayed in figure 4.12a. The axis-angle pair relating with these grains can also be represented as <-0.759 -0.503 0.411>/175°, and this is near Σ3 orientation relationship. Figure 4.13(a & b) shows the bright field and dark field transmission electron micrographs of two adjacent grains G and H. Figure 4.13 further reveals that these grains share the same zone axis <0 0 1>. The axis-angle pair relating to these grains can be represented equivalently by a rotation of 180° around <1.000 0.008 0.000>, and this is also near Σ3 orientation relationship.

From the results, obtained for orientation relationship between adjacent grains of alloy MA956, it is evident that the grains observed in the electron micrographs are not subgrain boundaries. Although many of the grains are close to Σ3 orientations, the deviation from Σ3 seems large enough to make the boundaries of the high energy type. This, together with the observations on the shape of the grains and their intense dislocation substructure is all consistent with a heavily deformed microstructure in the as-received condition. At this stage it seems reasonable to assume that the material contains significant amounts of energy stored in the form of dislocations and grain boundaries.

4.4 Conclusions

The nickel base superalloy MA6000 was received in the recrystallised condition, with a very small grain size (0.17μm), the grains being equiaxed in three dimensions. The grains contained few dislocations and exhibited annealing twins and clear sub-boundaries within the fine grains. On annealing, the alloy is expected to undergo secondary recrystallisation.

The ferritic steel MA956 was received in the cold deformed condition, with highly anisotropic rod like structure. The grains contained a high density of dislocations. The grains were found to be

relatively larger (0.45μm) in the as-received condition, and much of the stored energy is believed to be in the form of dislocations. During annealing, the alloy would be expected to undergo primary recrystallisation.

Table 4.1. Some coincidence site lattice (CSL) relations for cubic crystals, corrected from (Christian, 1965), after Bhadeshia (1987).

Σ	Angle	Axis	Twin axes
3	60.0	<1 1 1>	<1 1 1>, <1 1 2>
5	36.9	<1 0 0>	<0 1 2>, <0 1 3>
7	38.2	<1 1 1>	<1 2 3>
9	38.9	<1 1 0>	<1 2 2>, <1 1 4>
11	50.5	<1 1 0>	<1 1 3>, <2 3 3>
13a	22.6	<1 0 0>	<0 2 3>, <0 1 5>
13b	27.8	<1 1 1>	<1 3 4>
15	48.2	<2 1 0>	<1 2 5>
17a	28.1	<1 0 0>	<0 1 4>, <0 3 5>
17b	61.9	<2 2 1>	<2 2 3>, <3 3 4>
19a	26.5	<1 1 0>	<1 3 3>, <1 1 6>
19b	46.8	<1 1 1>	<2 3 5>
21a	21.8	<1 1 1>	<2 3 5>, <1 4 5>
21b	44.4	<2 1 1>	<1 2 4>

Table 4.2. Orientation relationship between two adjacent grains of ODS nickel base superalloy Inconel alloy MA6000 in as-deformed condition: axes are referred to the crystallographic basis and rotation operations are right handed. The sigma values are approximate.

No.	Adjacent Grains	axis-angle Pair				Σ
1	A-B	<0.000	0.608	0.793>	180°	3
2	C-D	<0.372	0.656	0.656>	180°	9
3	E-F	<0.618	-0.695	0.360>	160°	9
4	G-H	<0.553	0.622	0.553>	180°	3
5	I-J	<0.650	0.322	0.687>	154°	9
6	—	<0.777	0.629	0.000>	180°	3
7	—	<0.743	0.669	0.000>	180°	3
8	—	<0.687	0.650	0.322>	154°	9
9	—	<-0.435	0.676	0.593>	173°	9
10	—	<0.566	0.799	-0.200>	179.4°	13b
11	—	<0.268	-0.632	0.726>	168.5°	7
12	—	<0.332	0.609	0.719>	174°	9
13	—	<-0.792	0.297	-0.532>	179.6°	7
14	—	<0.302	-0.624	0.720>	156°	9
15	—	<0.596	-0.743	0.301>	176.2°	7
16	—	<0.928	0.263	0.263>	180°	9
17	—	<0.204	0.453	0.867>	174°	21b
18	—	<0.333	0.666	0.666>	180°	9
19	—	<-0.243	0.402	-0.882>	173.3°	21b
20	—	<0.167	-0.576	0.799>	177°	21
21	—	<-0.889	0.337	0.316>	177°	11
22	—	<-0.291	-0.698	-0.653>	164°	9
23	—	<-0.669	-0.246	0.700>	160°	19a
24	—	<0.323	0.669	0.669>	180°	9
25	—	<0.000	-0.707	-0.707>	178.5°	3
26	—	<0.591	0.716	0.255>	180°	7

51

Table 4.3. Orientation relationships between adjacent grains of ODS ferritic steel Incoloy alloy MA956 in the as-deformed condition: the axes are referred to a crystallographic basis, and rotation operations are right handed. The sigma values are approximate.

No.	Adjacent Grains	axis-angle Pair				Σ
1	A-B	<0.177	0.665	0.724>	180°	13b
2	C-D	<0.205	0.814	0.542>	180°	13b
3	E-F	<-0.759	-0.503	0.411>	175°	3
4	G-H	<1.000	0.008	0.000>	180°	3
5	—	<0.577	0.577	0.577>	180°	3
6	—	<0.429	0.386	0.816>	180°	3
7	—	<0.866	0.500	0.000>	180°	5
8	—	<0.764	0.644	0.000>	180°	3
9	—	<0.704	0.710	0.000>	180°	3
10	—	<0.714	0.699	0.000>	180°	3
11	—	<-0.418	0.741	-0.525>	176.4°	3
12	—	<0.744	0.312	0.589>	175°	9
13	—	<0.000	0.707	0.707>	180°	3
14	—	<0.007	1.000	0.000>	180°	3
15	—	<0.708	0.600	0.370>	163°	9
16	—	<0.697	-0.378	-0.608>	161.5°	9
17	—	<-0.661	-0.168	0.731>	174.3°	21a
18	—	<0.804	0.195	-0.561>	179°	13b
19	—	<0.704	0.428	0.566>	180°	3
20	—	<0.279	0.795	0.537>	180°	7
21	—	<0.402	0.414	0.816>	180°	3
22	—	<0.524	0.279	0.804>	180°	7
23	—	<0.516	0.289	0.805>	180°	7
24	—	<0.218	0.572	0.790>	180°	7